Research Paper

Stratigraphy and radiocarbon ages of late-Holocene Las Derrumbadas rhyolitic domes and surrounding vents in the Serdán-Oriental basin (Mexico): Implications for archeology, biology, and hazard assessment

Corentin Chédeville, [ID] Marie-Noëlle Guilbaud and Claus Siebe

Abstract

The Serdán-Oriental lacustrine basin in the eastern part of the Trans-Mexican Volcanic Belt holds a volcanic field of >30 monogenetic vents. Among them, the ~1000-m-high, ~11 km³ Las Derrumbadas rhyolite twin domes dominate the interior of the basin and are surrounded by smaller scoria cones, lava flows, shields, tuff rings, and maars. Of interest in this area are rare endemic species encountered in some of the maar lakes, as well as the large number of pre-Hispanic archeological sites indicating that the lacustrine environment became attractive as a dwelling hub during the late Holocene. We conducted a stratigraphic and radiocarbon dating study to reconstruct the volcanic history, assess the impact of past eruptions on the environment and pre-Hispanic populations, and evaluate future volcanic hazards. Accordingly, at least 10 volcanoes were identified to be < 25,000 BC of which eight are Holocene in age (Alchichica, Tecuitlapa, Atexcac, Cerro El Brujo, Tepexitl, Aljojuca, Derrumbadas, Piedras Negras). Hence, the central part of the Serdán-Oriental basin should be considered potentially active and new eruptions are likely to occur in the future. Furthermore, we show that the ~AD 20 Las Derrumbadas eruption is one of the most voluminous silicic effusive eruptions during the Holocene worldwide. This eruption possibly triggered a migration of human populations from dispersed rural hamlets in the central part of the basin toward fewer larger urban sites (e.g. Cantona) at its margins. Finally, the young ages of the maars imply that the unique biodiversity of their crater lakes must have developed over remarkably short timescales.

Introduction

In addition to a few dozen large stratovolcanoes and calderas, the Trans-Mexican Volcanic Belt (TMVB) includes several 1000 small- to medium-sized volcanoes whose ages range from early-Pleistocene to Holocene (Guilbaud et al., 2011, 2012; Hasenaka and Carmichael, 1985; Reyes-Guzmán et al., 2018; Siebe et al., 2005, 2004). In the eastern part of the TMVB, the Serdán-Oriental basin hosts a large number of vents encompassing the entire range of monogenetic volcano types encountered in the TMVB (maars, tuff rings/cones, scoria cones, lava flows, domes, and shield volcanoes; Figure 1). In the central part of the basin and culminating at ~1000 m above its floor, Las Derrumbadas rhyolite domes constitute a preeminent landmark (Figure 2). Yáñez-García and García Durán (1982) first dated Las Derrumbadas at 320 ka by the $^{40}K/^{40}Ar$ method. This date suggested that the volcanic landforms in the basin were relatively old, having thus little relevance in terms of volcanic hazards, which partly explains why the region had not received much attention from volcanologists until recently. However, based on morphological considerations, Siebe and Verma (1988) had already suggested that the domes might be younger than 40 ka. In later studies (e.g. Ort et al., 2009; Ross

et al., 2017; Zimmer et al., 2010), several other volcanoes in the area were dated by the $^{40}Ar/^{39}Ar$ method, yielding mainly late-Pleistocene ages (Table 1). More recently, Bernal et al. (2014) applied the $^{238}U/^{230}Th$ method to date zircons in lava blocks from the Las Derrumbadas domes, which produced a Holocene age, further confirming that the volcanic activity in the basin might be much younger than previously thought.

Although absolute dating techniques for volcanic rocks (e.g. $^{40}Ar/^{39}Ar$ and $^{238}U/^{230}Th$) have become increasingly precise for dating young samples (e.g. Renne et al., 1997; Yang et al., 2014), late Pleistocene and Holocene rocks often still remain difficult to date accurately. For instance, it can be occasionally troublesome to distinguish juvenile crystals from xenocrysts incorporated from

Departamento de Vulcanología, Instituto de Geofísica, Universidad Nacional Autónoma de México, Mexico

Corresponding author:
Corentin Chédeville, Departamento de Vulcanología, Instituto de Geofísica, Universidad Nacional Autónoma de México, Coyoacán, C.P. 04510 Ciudad de México, Mexico.
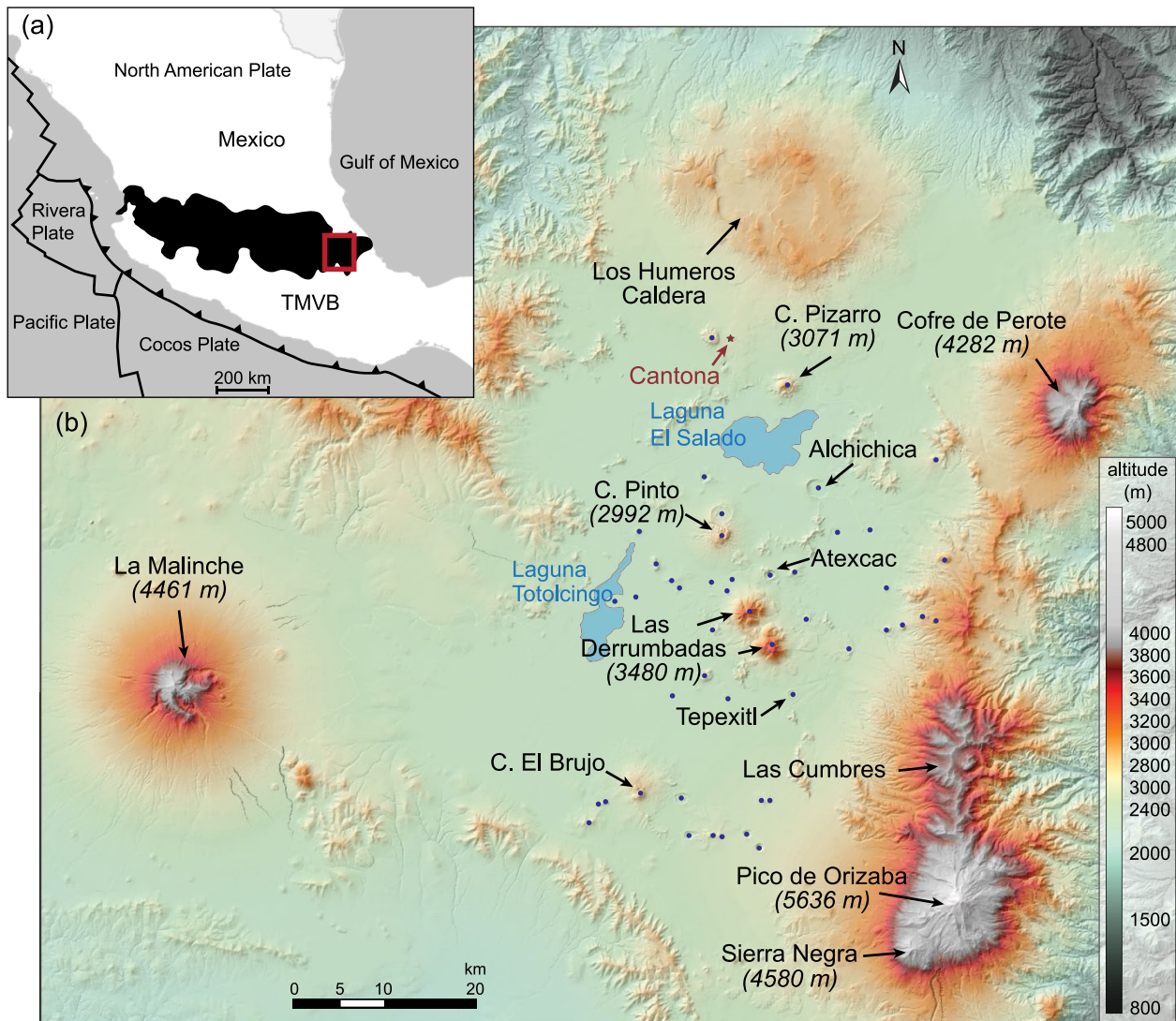Email: corentin.cm@gmail.com

Figure 1. (a) Location of the Serdán-Oriental basin (red quadrangle) within the Trans-Mexican Volcanic Belt (TMVB). (b) Location of volcanoes in the basin and along its margins. Blue dots indicate monogenetic vents in the interior of the basin. The archeological site of Cantona is also shown (red arrow).

an older, sometimes compositionally similar magma. Xenocrysts, if used in the analysis, would lead to overestimating the age of an eruption, an error that could be significant in the case of a very young event. It is thus legitimate to suspect that $^{40}K/^{40}Ar$ and $^{40}Ar/^{39}Ar$ ages reported for young volcanoes in the Serdán-Oriental basin (Table 1) might be too old and hence should be viewed with caution.

The possibility that volcanic activity could be much younger than previously thought would have important implications in regard to the most recent environmental history of the region. Volcanic hazards would need to be reassessed since a new eruption could be more likely to occur again in the future.

It is also known that human nomadic groups were present in central Mexico at least since the Pleistocene/Holocene boundary and the oldest settlements in the Serdán-Oriental basin date back to 1200 BC (Gazzola, 2005). Hence, the discovery of recent volcanic activity within the basin could have important archeological implications.

Another particularity of the basin is the rich and peculiar biodiversity present in some of the maar lakes that contain atypical, endemic flora and fauna (see details below). Dating these maars would provide important constraints on the timescales of colonization and species differentiation that took place in the recent past.

The main aim of this study was to reconstruct the chronology of the most recent period of volcanic activity in the central part of

the Serdán-Oriental basin. To fill this purpose, we conducted a detailed analysis of the volcanic stratigraphy in the area of Las Derrumbadas. We used the ^{14}C-dating method because it is relatively inexpensive, easy to implement, well constrained for young ages (<40,000 yr BP), and has provided reliable ages for young eruptions in México (Bloomfield, 1975; Carrasco-Núñez and Rose, 1995; Siebe et al., 1996, 2005, 2004). We report 23 radiocarbon ages that help constrain the age of eight different monogenetic edifices and discuss the discrepancies observed between our data and the previously published older ages. We also discuss the implications that such young ages (mainly Holocene) bear for past and future volcanic activity and its impact in this region, as well as for biological studies.

Geological, geographical, and biological setting

The TMVB is a late Tertiary-Quaternary arc related to the subduction of the Cocos and Rivera plates beneath the North American plate (Pardo and Suárez, 1995; Figure 1). The Serdán-Oriental tectonic basin forms an elevated lacustrine plain located in the eastern part of the TMVB. This endorheic basin covers an area of ~5000 km² and is bounded to the north by the Los Humeros caldera, to the southwest by La Malinche stratovolcano, and to the
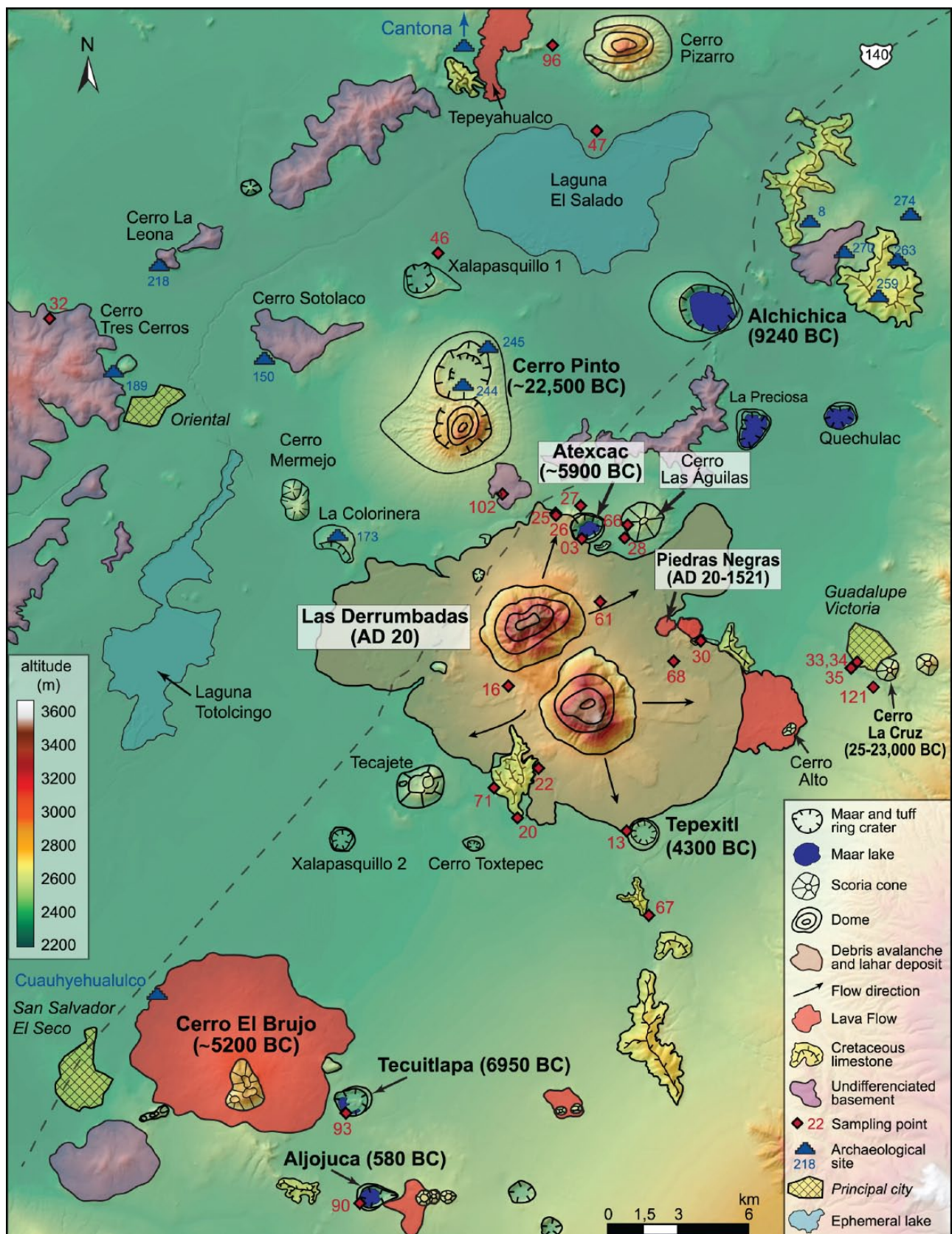
Figure 2. Geological map of Las Derrumbadas domes, surrounding volcanic edifices and basement structures. Calibrated radiocarbon ages are provided in parentheses. Archeological sites are indicated according to coordinates reported by Téllez-Nieto (2013). The archeological site of Cantona is located beyond the northern margin of the map, further north on the Tepeyahualco lava flow and its location is shown in Figure 1. Black dashed line represents federal road 140.

east by a N-S volcanic chain formed, from north to south, by Cofre de Perote, Las Cumbres, Pico de Orizaba (or Citlaltépetl) and Sierra Negra (Figure 1). Due to their relatively high elevations (4000–5700 m), these mountains experienced glacial activity during the coldest phases of the late Pleistocene as evidenced by

a series of moraines (Palacios and Vázquez-Selem, 1996; Vázquez-Selem and Heine, 2011).

The climate of the basin is temperate and subtropical, semi-arid to subhumid, with summer rains (average annual temperature = 12–16°C, annual total precipitation = 400–800 mm). The high

Table 1. Published radiometric ages for Las Derrumbadas and surrounding centers. Radiocarbon data are given in conventional and calibrated calendar ages.

Volcano	Age	Material dated	Method	Reference
Las Derrumbadas	320 ka	Dome rhyolite	$^{40}K/^{40}Ar$	Yáñez-García and García Durán (1982)
	4.7 + 1.3/−1.2 ka	Zircon in dome rhyolite	$^{230}Th/U$	Bernal et al. (2014)
Cerro Pinto	62 ± 8 ka	Sanidine crystal in dome rhyolite	$^{40}Ar/^{39}Ar$	Zimmer et al. (2010)
Tepexitl	29 ± 3.5 ka	Groundmass in rhyolite	$^{40}Ar/^{39}Ar$	Ross et al. (2017)
Aljojuca	5460 ± 25 yr BP (4260–4352 BC)	Pine pollen in lake sediment	^{14}C	Bhattacharya et al. (2015)
	2850 ± 30 yr BP (926–1109 BC)	Charcoal below pyroclastic sequence	^{14}C	De León-Barragán (2016)
Tecuitlapa	0.0 ± 20 ka	Groundmass in juvenile scoria cone clast	$^{40}Ar/^{39}Ar$	Ort and Carrasco-Núñez (2009)

volcanic mountains to the north and east create a rain-shadow effect over most of the basin, and xeric shrublands occupy the center of the basin. In its lowest parts (~2300 m a.s.l.), the basin contains two ephemeral alkaline playa lakes, Totolcingo (El Carmen) and Tepeyahualco (El Salado) (Figure 1), which remain dry for most of the year. In addition, maar lakes (locally called *axalapaxcos*), sustained by underground water (Ordóñez, 1905, 1906; Vilaclara et al., 1993), occur. Among them, lake Alchichica is the deepest natural lake (down to 66 m, Kaźmierczak et al., 2011) in Mexico, and is both brackish and alkaline (pH ~9). It is ecologically unique with stromatolite deposits (Couradeau et al., 2012; Gérard et al., 2013; Kaźmierczak et al., 2011) and the presence of a diversified endemic biota that adapted to the extreme aquatic conditions and which include species of diatoms (Oliva et al., 2006), crustaceans (Escobar-Briones and Alcocer, 2002; Montiel-Martínez et al., 2008; Suárez-Morales et al., 2013), insects (Acosta et al., 2017; Jansson, 1979), fish (de Buen, 1945), as well as salamander (Brandon et al., 1981).

Elongated topographic landforms within the basin consist of Upper Cretaceous marine sediments (mostly limestones) that were folded and faulted during the Laramide orogenesis and represent a >1000-m-thick basement in the area (Yáñez-García and García-Durán, 1982). During the Tertiary, these limestones were intruded by small monzonite and granodiorite plutons and associated dikes, generating contact metamorphism and hydrothermal mineralization, as evidenced by the presence of skarns and marbles (Yáñez-García and García-Durán, 1982), and associated sulfide-ore veins (Burkart, 1867). Terrigenous sedimentation started at the end of the Tertiary and has continued during the Quaternary, depositing conglomerates, sands, and lacustrine clays in the basin (Yáñez-García and García-Durán, 1982). In the Pleistocene, intense volcanic activity formed a high diversity of volcanic landforms ranging from small-volume basaltic to rhyolitic scoria cones, maars, tuff rings, tuff cones, and lava flows, to prominent rhyolitic domes (Carrasco-Núñez et al., 2012; Negendank et al., 1985; Yáñez-García and García-Durán, 1982) (Figure 1). Eventually, the intermontane basin became closed, probably as a result of this activity, although this important issue has never been addressed.

Las Derrumbadas and surrounding centers

Surprisingly, few studies have been conducted on the Las Derrumbadas domes and their eruptive mechanisms remain poorly understood. One of their most remarkable features is the instability of their slopes that are affected by frequent rockfall (*derrumbes*, in Spanish, from where the name *Derrumbadas* derives) whose deposits are subsequently mobilized by lahars during the summer rainy season. Debris avalanche deposits, which are commonly associated with the collapse of large parts of volcanic edifices (van Wyk de Vries and Davies, 2015), are also found at the base of the domes (Figure 2; Siebe et al., 1995). The summit of the southeastern dome displays fumarolic activity, which explains the interest in this area for geothermal prospection (Siebe and

Verma, 1988; Yáñez-García and Casique, 1980; Yáñez-García and García-Durán, 1982).

At least 25 additional volcanic edifices are present in a 15-km-radius around Las Derrumbadas (Figure 2). These include maars and tuff rings (Atexcac, Alchichica, Tepexitl, Xalapasquillo 1 and 2, La Preciosa, Quechulac, Toxtepec, La Colorinera), scoria cones (Cerro La Cruz, Cerro Las Águilas, Cerro Alto, Tecajete, Cerro Mermejo, and several unnamed smaller ones), one tuff ring/dome complex (Cerro Pinto), and a blocky lava flow without cone at its source (Piedras Negras). Among these, only Atexcac (Carrasco-Núñez et al., 2007), Cerro Pinto (Zimmer et al., 2010), and Tepexitl (Austin-Erickson et al., 2011; Ross et al., 2017) have been studied individually in detail. However, these studies focused on the characteristics of proximal deposits to reconstruct the dynamics of the eruptions, and do neither report tephra-fallout isopach maps, nor establish the time and stratigraphic relation between products from the different volcanoes. Although Alchichica has been investigated extensively by biologists and limnologists (see previous section), geological studies are still notably absent. Twenty kilometers southwest of the Las Derrumbadas domes are three additional volcanoes, including a lava shield (Cerro El Brujo) and two maars (Aljojuca and Tecuitlapa) that display well-preserved morphologies indicative of young ages. Tecuitlapa and Aljojuca maars were studied by Ort and Carrasco-Núñez (2009) and De León-Barragán (2016) respectively.

Methods

The stratigraphic and geomorphological relations between the youngest edifices in the study area were established through extensive fieldwork, complemented with the interpretation of aerial photographs, and satellite images on which the geologic map (Figure 2) is based. We studied thick vertical sections exposed along road and river cuts and inside quarries, where the deposits of several volcanoes could be found, separated in most cases by paleosols. Recognizable pumice and tephra layers in the area were used as marker beds to correlate between the different stratigraphic sections. The age of the different edifices was constrained by collecting samples of paleosols located just below associated pyroclastic deposits, carefully selecting sections where the paleosol and the tephra showed no or little evidence for post-depositional reworking (e.g. flat, horizontal, and sharp interface between both products, laminations in fallout tephra, absence of incorporation of paleosol in the tephra). In addition, we controlled that the pre-existing topography was flat so that the paleosol had undergone limited erosion before and during deposition of the overlying tephra. The validity of the obtained ages was verified carefully using the reconstructed stratigraphy and morphological considerations (see further information in the 'Results' section for each case).

Paleosols were carefully sampled in their uppermost 2 cm in order to obtain the closest age possible for the overlying deposit (Matthews, 1985). In two cases (samples 22A and 90A), few mm to 1 cm long charcoal fragments, found within the upper 5 cm of the paleosol, were collected and dated, and, in another case,

fragments from partly charred, several-cm-long wood pieces found directly within the deposits, were utilized. When present, charcoal was preferred to bulk paleosol samples, as it is generally less subject to contamination (Matthews, 1985).

The samples were sent to Beta Analytics Inc. (Florida, US) where they were submitted to standard pretreatment protocols (see details on the website of Beta Analytics laboratory). All samples were dated by the accelerator mass spectrometry (AMS) method, except in the case of partially charred wood, which was dated by radiometric detection because of its larger size (100 g). The conventional ages (including those from other studies) were calibrated by reference to the IntCal13 database (Reimer et al., 2013).

The usefulness of the radiocarbon method to date volcanic eruptions mostly relies on the correct identification of the source of the deposits below or within which the organic material is collected. For this reason, we studied in detail the characteristics of the deposits, comparing them to proximal products and published data. For granular deposits, the coarsest fragments (down to coarse ash) were first identified directly in the field with a hand lens and HCl, in order to distinguish between, for example, dense rhyolitic glass and chert and/or micritic gray limestone fragments that are often similar in aspect and color. Then, representative bulk samples were sieved in the Laboratory of Volcanic Sedimentology at the Instituto de Geofísica (IGF, UNAM, Mexico), and their components were identified under a binocular microscope. To identify minerals with more precision, high quality polished thin sections were made of some of the products (lavas, scoria, and basement rocks), and the thin sections were observed under the petrographic microscope at IGF, UNAM. Some unidentified minerals (mainly oxides) and fragments were also analyzed using a Scanning Electronic Microscope (SEM, Zeiss EVO MA10) at Instituto de Geología, UNAM, Mexico.

Results

The main result of this study is the reconstruction of the volcanic stratigraphy in the central part of the Serdán-Oriental Basin for the last 27,000 years. The 23 main stratigraphic sections on which our interpretations are based are included in the Supplementary Material 1 (available online). The obtained radiocarbon ages are listed in Table 2 and reported in the text as calibrated calendar (AD or BC) ages. Stratigraphic sections that were particularly important for reconstructing the stratigraphy in this area are reproduced in Figure 3 and a composite stratigraphic section is presented in Figure 4. Photographs showing the morphology of the dated volcanoes are shown in Figure 5. We now describe in stratigraphic order each of the dated deposits, starting from the oldest (bottom) of the sequence to the youngest (upward).

Quetzalapa Pumice

The oldest radiocarbon-dated deposit in the study area corresponds to the so-called Quetzalapa Pumice that crops out along the eastern margin of the basin, on the west-facing slopes of the Las Cumbres Volcanic Complex (Figure 1; see also Rodríguez et al., 2002). This deposit was dated at ~23,000 yr BP (~25,000 BC) by averaging several ages of soil and charcoal fragments collected in a paleosol and an ash-flow deposit located immediately below the main pumice fallout deposit (Rodríguez, 2005; Rodríguez et al., 2002).

The Quetzalapa Pumice deposit was observed in the easternmost part of the study area, at site 121 and close to site 35, near the town of Guadalupe Victoria where it is >4 m thick (Figures 2 and 4, Supplementary Material 1, available online). Juvenile fragments mainly consist of light brown to white, moderately to highly vesicular rhyolitic pumice, rich in small biotite crystals (<2 mm). Lithics consist mostly of andesitic lava and lesser

amounts of hydrothermally altered fragments. The deposit consists of a thick, massive, well-sorted, clast-supported white pumice fallout layer overlain by thinner, laterally dicontinuous, matrix-supported, poorly sorted layers rich in lithics (pyroclastic flows and/or lahars). The characteristics and thickness of the deposit coincide with those reported by Rodríguez et al. (2002).

Cerro La Cruz scoria cone

The next volcano in the stratigraphy is Cerro La Cruz, a 150-m-high scoria cone located at the eastern border of the study area (Figures 2 and 5a). This volcano fed an olivine-bearing lava flow that, at site 33, directly covers a coarse, 1.3-m-thick dark-gray scoria fallout deposit also rich in olivine (Supplementary Material 1, available online). The lack of soil development between the scoria fallout and the lava and their similarity in mineralogy both indicate that the scoria also originated from Cerro La Cruz, consistent with its coarseness (lapilli) and the decrease of thickness of the deposit away from the cone (at site 35, it is only 85 cm thick).

This scoria fallout lies above a brown, poorly sorted, slightly indurated, matrix-rich deposit with rounded pumices and lithics interpreted as reworked material from the underlying Quetzalapa Pumice. Two samples from deposits at sites 33 and 35 had too low carbon content (<0.05%) for reliable dating. The stratigraphic position of the scoria above the Quetzalapa Pumice however indicates that it must be younger than 25,000 BC.

White pumice fallout deposit from unknown source

The following stratigraphic layer is a 25-cm-thick well-to-moderately sorted pumice fall deposit that overlies the Cerro La Cruz scoria fallout with a 12-cm-thick paleosol at site 33 (Figure 2 and Supplementary Material 1, available online). Pumice clasts are sub-angular, up to 2 cm in maximum diameter, and moderately to highly vesiculated with vesicles mostly of sub-rounded shape and rarely fibrous in texture. Phenocrysts consist mainly of plagioclase and hornblende with possibly few pyroxenes and scarce biotite. This pumice fallout is typical of products from Plinian or sub-Plinian eruptions from stratovolcanoes or calderas. Based on their proximity, we consider several volcanoes as a potential source: Las Cumbres (~20 km), Pico de Orizaba (~30 km), los Humeros (~40 km), and La Malinche (~70 km). Given the estimated age of the fallout between 25,000 and 22,500 BC (see Figure 4), Las Cumbres, Pico de Orizaba, and los Humeros could be discarded since Plinian eruptions of that age range have not been reported from these sources (Carrasco-Núñez et al., 2018; Ferriz and Mahood, 1984; Hoskuldsson and Robin, 1993; Rodríguez, 2005). Instead, a pumice fallout from La Malinche has been radiocarbon dated at ~21,500 yr BP (~23,500 BC; Castro-Govea and Siebe, 2007). Their description of the pumice clasts (whitish with phenocrysts of plagioclase, hornblende, clinopyroxene, ortopyroxene, and biotite) coincides with our deposit, which makes it a likely candidate, although this still requires further confirmation by geochemical data and other means.

Cerro Pinto tuff ring-dome complex

Deposits from Cerro Pinto, two imbricated tuff rings with the southern one hosting a series of small domes (Zimmer et al., 2010; Figures 2 and 5b), were observed across the study area, ranging from >8 m to 55 cm in thickness and reaching up to 18 km from the vent. They are easy to identify by their bright-white color that stems from their abundance in poorly crystalline and finely vesicular white pumice (see below). At medial distances from the vent (sites 3, 8 and 102), the deposits consist mostly of partly indurated, fine to medium ash, moderately sorted layers with cross-and-wavy to planar stratification, intercalated with some coarser and better-sorted ash to fine lapilli planar layers, which we interpret as

Table 2. New radiocarbon ages (this study) for Las Derrumbadas and surrounding monogenetic volcanoes (in stratigraphic order).

Origin	Sample no.	BETA analytic lab. no.	Conventional age (yr BP)	Calendar calibration (2σ)	Average calendar age (2σ)	Calibration (2σ) (yr BP)	Average calibrated age (2σ) (yr BP)	IRMS d13C o/oo
Derrumbadas late lahar	16 H[a]	466697	960 ± 30	AD 1020–1155	AD 1090	930–795	860 ± 70	−23.9
Derrumbadas avalanche	22A[b]	466699	1970 ± 30	45 BC–AD 85	AD 20	1994–1865	2930 ± 70	−21.1
	13B	466696	2360 ± 30	(94.2%) 522–383 BC (1.2%) 536–528 BC	460 BC	(94.2%) 2471–2332 (1.2%) 2485–2477	2410 ± 80	−24
Derrumbadas surges	66G	481591	2300 ± 30	(79.6%) 407–356 BC (15.8%) 287–234 BC	320 BC	(79.6%) 2356–2305 (15.8%) 2236–2183	2270 ± 90	−19.5
	26A	471553	2480 ± 30	(94.9%) 774–482 BC (0.5%) 441–434 BC	600 BC	(94.9%) 2723–2431 (0.5%) 2390–2383	2550 ± 180	−24.9
	30A	481581	2490 ± 30	781–511 BC	650 BC	2730–2460	2600 ± 140	−20.2
	28A	466701	3010 ± 30	(78.9%) 1310–1157 BC (12.2%) 1386–1340 BC (4.4%) 1147–1128 BC	1260 BC	(78.9%) 3259–3106 (12.2%) 3335–3289 (4.4%) 3096–3077	3210 ± 140	−21.1
	20A	466698	3200 ± 30	1526–1417 BC	1470 BC	3475–3366	3420 ± 60	−22.2
	71A	481593	3880 ± 30	(94.2%) 2467–2286 BC (1.2%) 2247–2236 BC	2350 BC	(94.2%) 4416–4235 (1.2%) 4196–4185	4300 ± 120	−21.7
Aljojuca	90A[b]	492706	2430 ± 30	(69.2%) 590–405 BC (19.6%) 750–683 BC (6.6%) 668–639 BC	580 BC	(69.2%) 2539–2354 (19.6) 2699–2632 (6.6%) 2617–2588	2620 ± 80	−23.2
Tepexitl	67A	481592	5450 ± 30	4351–4255 BC	4300 BC	6300–6204	6250 ± 50	−21.5
Cerro El Brujo	156	526394	5960 ± 30	(94.5%) 4936–4769 BC	4840 BC	(94.5%) 6885–6718 cal. BP (0.9%) 6702–6695 cal. BP	6790 ± 100	−22.3
	173	526395	6650 ± 30	(0.9%) 4753–4746 BC	5580 BC	7580–7475 cal. BP	7530 ± 60	−20.9
Atexcac	25A	466700	4420 ± 30	(82.7%) 3115–2921 BC (7.1%) 3266–3236 BC (5%) 3321–3272 BC (0.6%) 3171–3163 BC	3120 BC	(82.7%) 5064–4870 (7.1%) 5215–5185 (5%) 5270–5221 (0.6%) 5120–5112	5070 ± 200	−21.3
	66A	481589	6470 ± 30	5484–5372 BC	5430 BC	7433–7321 cal. BP	7380 ± 60	−21.6
	03D	464875	7480 ± 30	(62.7%) 6427–6331 BC (32.7%) 6317–6253 BC	6340 BC	(62.7%) 8376–8280 (32.7%) 8266–8202	8290 ± 90	−16.5
Tecuitlapa	93A	492705	8040 + /−30	(72.3%) 7073–6910 BC (23.1%) 6886–6829 BC	6950 BC	(72.3%) 9022–8859 (23.1%) 8835–8778	8900 ± 130	−17.7
Alchichica	46B	481586	1250 ± 30	(74.8%) AD 676–779 (20.6%) AD 790–870	AD 770	(74.8%) 1274–1171 (20.6%) 1160–1080	1180 ± 100	−21
	47A	481587	9750 ± 30	9286–9201 BC	9240 BC	11,235–11,150	11,190 ± 50	−21.8
Cerro Pinto	96E	492704	11,360 ± 40	11,344–11,159 BC	11,250 BC	13,293–13,108	13,200 ± 100	−19.3
	32A	466702	19,820 ± 60	22,130–21,680 BC	21,910 BC	24,079–23,629	23,850 ± 230	−22.3
	102A	515745	21,250 ± 60	23,842–23,439 BC	23,640 BC	25,791–25,388	25,590 ± 210	−19.1
Lake sediments within Las Derrumbadas debris avalanche block	8740	8740	31,140 + 1075/−945	35,940–31,072 BC	33,500 BC	37,890–33,022	35,450 ± 2450	−24.1

[a]Partially charred wood; [b]Charcoal.

products from pyroclastic surges and fallout, respectively. At distal site 96, the deposit consists at its base of loose, clast-supported, well-sorted, very coarse ash with sub-angular to angular fragments, overlain by stratified, indurated fine ash. In comparison, at distal sites 32 and 34, the deposits are mostly massive, moderately to well-sorted fine ash deposited by fallout.

Clasts mainly consist of white, sub-angular to angular, finely to moderately vesiculated (60–70 vol%) rhyolitic pumice with plagioclase and subeuhedral biotite (typically <250 μm). In fine fractions (2 phi) some fragments are dense and translucid (glass shards). Most of the pumices and glass shards enclose tiny (<10 μm) blackish crystals that might be small biotites. In thin sections, the vesicles in the pumices appear strongly elongated in one direction (typically parallel to the grain long axis) and are often curved. The deposit also contains lesser amounts of stony (dense and microcristalline) rhyolite with the same mineralogy as the pumices and a color varying from light gray to gray, to greenish. Lithics consist principally of micritic limestone of two types: (1)
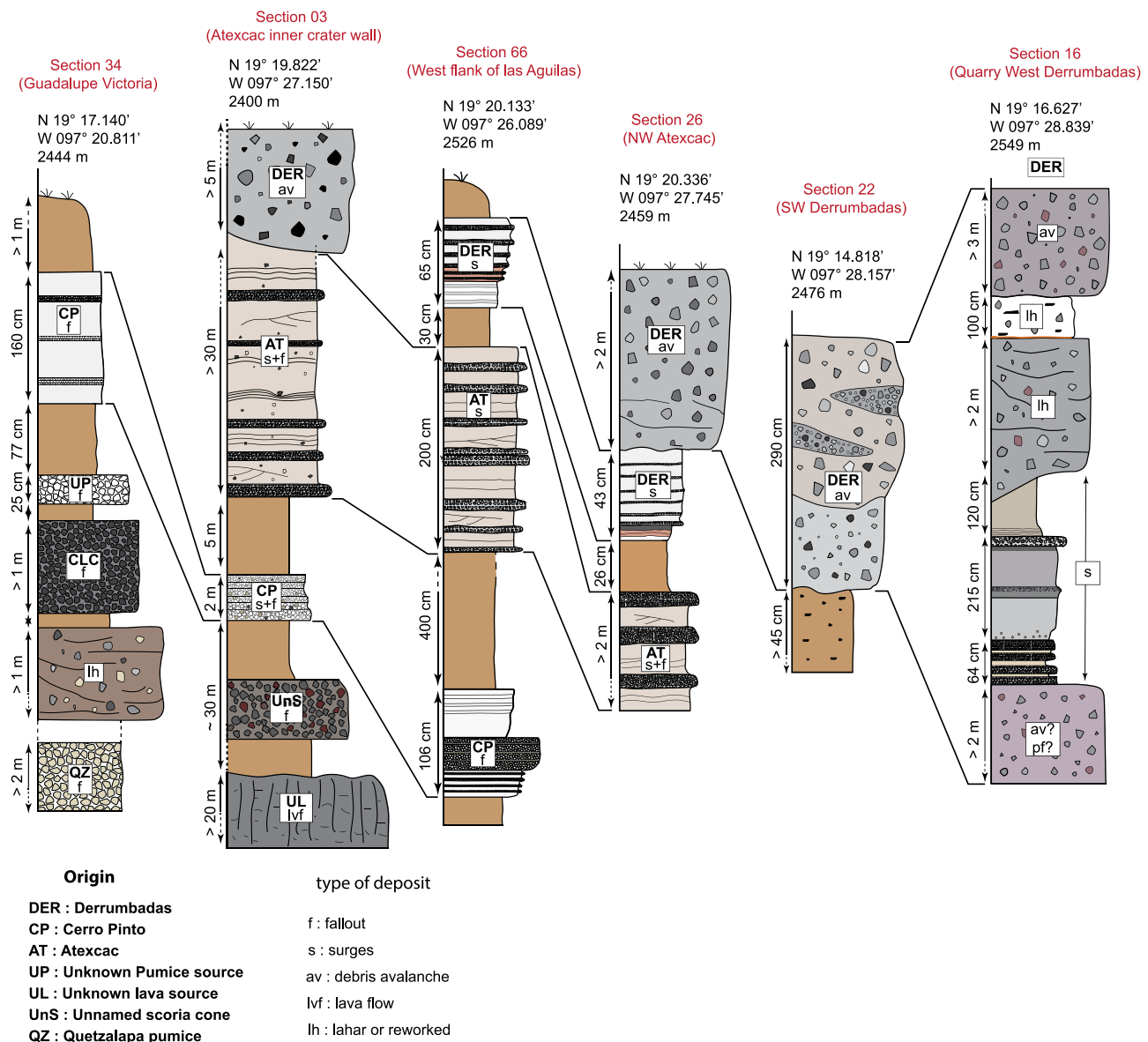
Figure 3. Stratigraphic correlation of recent volcanic deposits in the studied area (selected stratigraphic sections). See radiocarbon data in detailed sections in Supplementary Material 1 (available online) and Figure 4.

brown-beige, sub-angular to sub-rounded, and slightly translucid and (2) dark, sub-rounded, and completely opaque. There are also rare fragments of monzonite that contain orthoclase, plagioclase, and biotite. At fine fractions (2 phi) free crystals are mainly plagioclase with lesser biotite, quartz, and few hornblende. All these characteristics are in agreement with descriptions of the Cerro Pinto proximal facies, labeled Tp and Tpb by Zimmer et al. (2010). At sites 3, 32, and 34 some translucent-green, prismatic crystals were also observed. In thin sections, these are colorless with medium relief, and their interference colors range from the middle first order to the low second order.

Six paleosols below the deposits at sites 3, 32, 33, 35, 96, and 102 were radiocarbon dated but three of them did not yield an age due to low carbon content (<0.05%). Notably, the basal contact of the deposits were in all places irregular and mixed with an underlying, poorly developed paleosol poor in organic matter. The paleosols at sites 32, 96, and 102 yielded ages of 21,910 BC, 11,250 BC, and 23,640 BC, respectively. All these ages are consistent with the stratigraphy and other radiocarbon ages (Figure 4), but the age from site 96 seems anomalous since it is much younger than the two others. We thus propose an age of ~22,500 BC for Cerro Pinto.

Alchichica tuff ring or maar

The next volcano higher up in the stratigraphy is the Alchichica maar that is located in the NE sector of the study area, ~10 km east of Cerro Pinto (Figure 2). Its crater is 1.9–2.4 km in diameter (rim to rim) and its depth from the rim to the lake surface varies from 25 m on the east to 170 m on the west side, where an older scoria cone is exposed (Figure 5c). Proximal deposits from this volcano are exposed in the maar inner crater walls. They consist of gray to dark gray, well-stratified, cross-bedded layers that are strongly deformed by ubiquitous bomb impact sags. Layers range from fine ash, indurated, and rich in accretionary lapilli, to friable coarse ash to fine lapilli. Juvenile clasts consist of mafic dark scoria with small irregularly shaped vesicles and phenocrysts of mainly plagioclase and fewer pyroxenes. Juvenile fragments are relatively abundant (10–30 vol%) in fine fractions but rare as blocks. Lithics consist principally of dark-gray lava clasts that are dense or display round vesicles, with lesser amounts of fine-grained limestone with a notable variety of colors (brown-beige, yellowish, red-orange, gray, and dark gray), oxidized red and dark-gray clasts, and hydrothermally altered ochre-red fragments. There are also some gray dense rhyolite clasts and white pumices with elongated vesicles, both of which contain plagioclase and
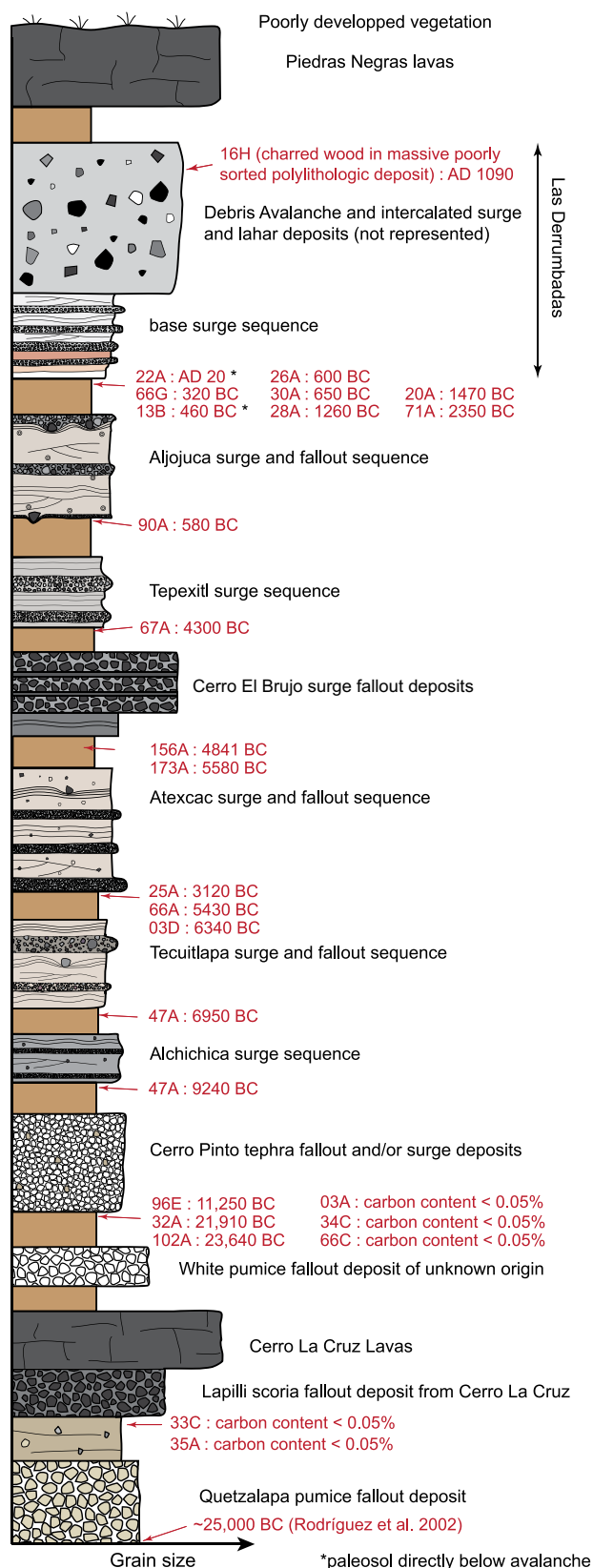
Poorly developed vegetation

Piedras Negras lavas

16H (charred wood in massive poorly sorted polylithologic deposit) : AD 1090

Debris Avalanche and intercalated surge and lahar deposits (not represented)

Las Derrumbadas

base surge sequence

22A : AD 20 *   26A : 600 BC
66G : 320 BC   30A : 650 BC   20A : 1470 BC
13B : 460 BC *   28A : 1260 BC   71A : 2350 BC

Aljojuca surge and fallout sequence

90A : 580 BC

Tepexitl surge sequence

67A : 4300 BC

Cerro El Brujo surge fallout deposits

156A : 4841 BC
173A : 5580 BC

Atexcac surge and fallout sequence

25A : 3120 BC
66A : 5430 BC
03D : 6340 BC

Tecuitlapa surge and fallout sequence

47A : 6950 BC

Alchichica surge sequence

47A : 9240 BC

Cerro Pinto tephra fallout and/or surge deposits

96E : 11,250 BC   03A : carbon content < 0.05%
32A : 21,910 BC   34C : carbon content < 0.05%
102A : 23,640 BC   66C : carbon content < 0.05%

White pumice fallout deposit of unknown origin

Cerro La Cruz Lavas

Lapilli scoria fallout deposit from Cerro La Cruz

33C : carbon content < 0.05%
35A : carbon content < 0.05%

Quetzalapa pumice fallout deposit

~25,000 BC (Rodríguez et al. 2002)

Grain size   *paleosol directly below avalanche

Figure 4. Composite stratigraphic section for eruptions of the last 27,000 years in the study area. All ages reported on the figure are calibrated calendar ages.

biotite, similar to Cerro Pinto products. Distal deposits from this maar were found covering low-sloping hills made by older volcanoes at a distance of 8 and 10 km from the source at sites 46 and 47 (Figure 2), respectively. These deposits are dark gray, indurated, cross-bedded, fine-grained, and rich in accretionary lapilli (Supplementary Material 1, available online), as is typical for the

distal facies of base surges associated to phreatomagmatic eruptions (Wohletz and Sheridan, 1979). The relatively large horizontal distance reached by the surges can be explained by the flatness of the terrain and the absence of topographical obstacles around the maar (Figure 2). Other possible sources for these surges were discarded on the basis of composition (Cerro Pinto and Jalapasquillo 2 are rhyolitic and produced whitish deposits), morphology (La Preciosa and Quechulac mafic maars show more degraded morphologies that suggest older ages), and both composition and age (Cerro Pizarro dome is rhyolitic and older than 60 ka, Carrasco-Núñez and Riggs, 2008).

The paleosol samples below the distal surges gave ages of AD 770 and 9240 BC, respectively. Dating of emerged stromatolite deposits within the Alchichica crater by Kaźmierczak et al. (2011) gave an age of 2.8 ± 0.31 ka (^{238}U/^{230}Th), which indicates that the maar must be significantly older than 1000 BC, and that the AD 770 paleosol is probably contaminated with recent carbon. The older radiocarbon age (9240 BC) is consistent with the somewhat eroded morphology of the maar crater that displays gentler inner slopes and deeper gullies, in comparison to the steeper slopes of younger maars such as Atexcac and Aljojuca (see below).

Tecuitlapa

The Tecuitlapa maar is located in the southern part of the basin. It forms an E-W elongated tuff ring that ranges between 1.1 and 1.4 km in diameter and 70 and 100 m in depth. The crater is partly filled by late-erupted scoria and spatter cones that are surrounded on one side by a half-moon shaped small lake (Figure 5d; Ort and Carrasco-Núñez, 2009). The crater walls expose the contact of the phreatomagmatic sequence with the paleosurface that consists of an ashy light-brown deposit called 'toba café' by Ort and Carrasco-Núñez (2009). Dating of a bulk sample from this paleosol yielded an age of 6950 BC. This relatively young age is consistent with the steepness of the crater walls. The crater-diameter/crater-depth ratio is quite high (>14) for such a young crater (Pirrung et al., 2008; Wood, 1974) but this can be explained by its larger than usual diameter caused by a fissure vent, and by its relatively shallow depth caused by the partial filling of the crater by the late scoria cones.

Atexcac maar

Atexcac maar is located 4 km northeast of the northwest dome of Las Derrumbadas (Figure 2). The crater diameter ranges between 850 and 1150 m and its depth varies from ~80 m on the SE to >200 m on the NW, from the rim to the surface of the lake, which is about 40 m deep (Carrasco-Núñez et al., 2007). Similar to Alchichica, the crater cuts into an older scoria cone that is partly exposed on the NW inner crater walls and that overlies a folded limestone relief from the basement, while a pre-existing olivine-rich lava is visible on the S and W walls (Figure 5e). The inner crater walls also expose Atexcac's proximal sequence of deposits (~60 m thick) consisting of gray, friable, planar-bedded, lapilli layers alternating with gray-beige, fine-to-very fine ash layers showing cross-bedding and wavy stratification (see also Carrasco-Núñez et al., 2007). Large (>50 cm) ballistic blocks are common and associated with impact sags. Juvenile clasts are dark-gray vesiculated scoria with phenocrysts of plagioclase (various with sub-rounded shape), fewer pyroxene and hornblende phenocrysts, microlites of olivine, and small (2–3 mm) white xenoliths (plagioclase or zeolites). Lithic clasts are mostly fragments of dark vesicular lava, gray-beige limestone, red oxidized scoria with well-rounded vesicles, and whitish-greenish-yellowish skarn-xenoliths with andradite garnet and Ca-Mg pyroxenes (wollastonite and diopside). The abundance of juveniles strongly varies vertically within the deposit (Carrasco-Núñez et al., 2007)
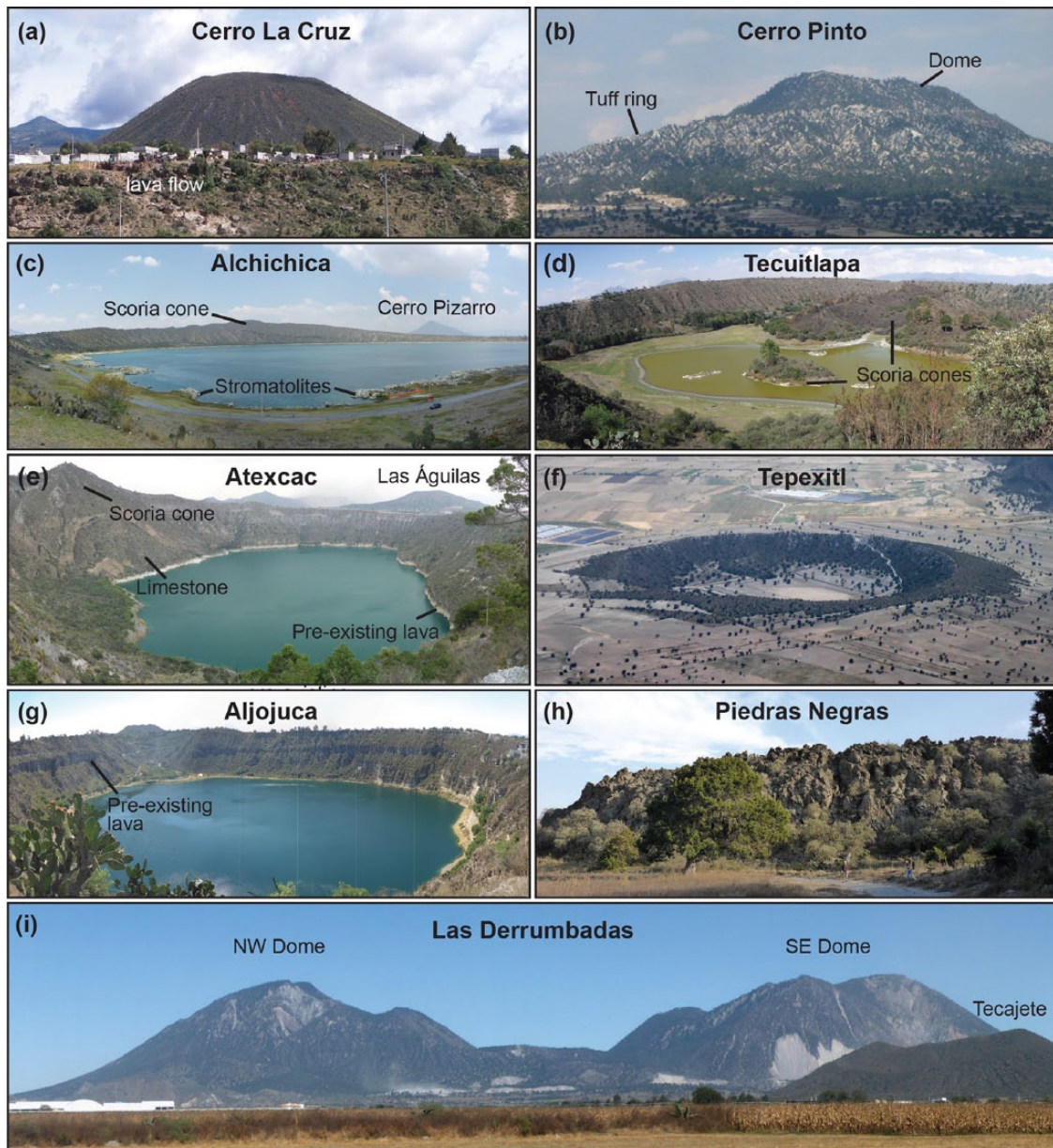
Figure 5. Photographs of late Pleistocene–Holocene monogenetic volcanoes dated in this study.

and juvenile bombs are particularly common at the upper part of the section. Medial deposits (sites 25 and 26) show similar alternations between coarse and fine layers, and an abundance of micro-vesicular dark-gray juvenile clasts in the upper layers, that distinguishes them from products of other maars (Figure 3 and Supplementary Material 1, site 25, available online). The deposits show a rapid decrease in thickness and grain size with distance from the source.

The stratigraphic relation of Atexcac maar deposits above Cerro Pinto and below Las Derrumbadas products is well exposed in the inner crater walls (site 03, Figure 3 and Supplementary Material 1, available online; see also Carrasco-Núñez et al., 2007). There, a 4-m-thick paleosol separates Cerro Pinto fallout and surge deposits (below) from the Atexcac phreatomagmatic surge sequence (above), suggesting that a relatively long time (probably several 1000 years) elapsed between the two eruptions. A debris avalanche from Las Derrumbadas, rich in obsidian and limestone clasts, covers, with an erosive lower contact, the maar deposits at the southern rim of the crater (see also Carrasco-Núñez et al., 2007).

Paleosols below Atexcac surges were dated at 3120 BC, 5430 BC, and 6340 BC respectively (Figure 4). All these ages are younger than Alchichica, which is consistent with the steeper maar crater walls of Atexcac and stratigraphic observations. Of the three radiocarbon ages, one seems anomalously young (3120 BC) while the two others (5430 and 6340 BC) are similar. We thus estimate the age of Atexcac at ~5900 BC.

Cerro El Brujo lava shield

Cerro El Brujo volcano is located in the southern part of the study area (Figure 2). It is the largest mafic volcanic edifice in the basin, and forms a lava shield that is ~9 km in diameter and crowned by a cluster of scoria cones with pristine craters. The lava shield covers the western flank of the Tecuitlapa maar and is not overlain by tephra from this maar, which indicates that it is younger. The eruption of Cerro El Brujo started by a complex sequence of surge and fallout tephra deposits below which paleosols were sampled at two locations. These gave consistent ages of 4840 BC (site 156) and 5580 BC (site 173), suggesting an age of ~5200 BC for this eruption, in agreement with the older age of Tecuitlapa reported above (6950 BC).

Tepexitl tuff ring

Tepexitl tuff ring is located southeast of Las Derrumbadas (Figure 2). Its crater is ~1 km in diameter and up to 75 m deep

(Figure 5f). Observing proximal deposits exposed at the crater walls, Austin-Erickson et al (2011) describe distinct types of layers that can be subdivided into (1) gray, loose, massive, poorly sorted coarse ash to fine lapilli; (2) white to light gray, cross-stratified ash with occasional accretionary lapilli; and (3) fines-depleted, clast-supported lapilli breccia. The lower part of the sequence is finer grained and strongly deformed by bomb sags whereas the upper part is coarser grained and rarely displays bomb sags. Medial deposits (site 19, 1.5 km SW of maar center) show an alternation of thick, gray-beige, fine-to-very fine ash layers with wavy and cross-stratification, and thinner, light gray stratified layers of coarse ash to medium lapilli. Three kilometers south from the source (site 67, Figure 2), the distal deposits are 60 cm thick and consist of indurated, white fine ash rich in accretionary lapilli with a gray coarse-ash layer toward the top. In this coarse layer, juvenile clasts mostly consist of poorly to moderately vesiculated, light-gray to gray rhyolite, light-gray pumices (more abundant in fractions >0 phi) and obsidian, all with abundant phenocrysts of plagioclase, K-feldspar, biotite, fewer quartz, and rare small (<250 μm) garnet (almandine), in general agreement with descriptions of proximal juvenile clasts by Austin-Erickson et al. (2011).

The paleosol directly underlying distal Tepexitl deposits was dated at 4300 BC. This young radiocarbon age appears to be, on the one hand, inconsistent with the somewhat eroded morphology of the tuff ring that does not host water and is shallower (50–70 m) than Atexcac (Figure 5f). On the other hand, it agrees with the lack of soil development on top of the tuff ring (Figure 3 in Austin-Erickson et al., 2011). Also, its more eroded slopes may have resulted from the friable nature of its proximal deposits in comparison to those of Atexcac, which are indurated finer grained surge deposits that are more resistant to erosion.

Aljojuca

Aljojuca maar has an E-W elongated crater whose diameter ranges from 1 km in a N-S to 1.5 km in an E-W direction. It contains a 30-m-deep lake in its interior and its sub-vertical crater walls expose >50 m of pre-existing deposits (Figure 5g). The basal contact of the phreatomagmatic sequence is exposed around the entire crater and shows a light-brown sandy deposit containing small-sized pumice and lithic clasts ('toba café') underlying the maar deposits. Centimeter-sized charcoal fragments found 1–2 cm below the contact were dated at 580 BC, which is consistent with the age reported by De León-Barragán (2016) obtained on similar material (~1000 BC).

Sediments at the bottom of the crater lake were studied by Bhattacharya et al. (2015) who dated organic material (charcoal, wood fragment, pollen) preserved in layers recovered from drill cores at various depths. The reported ages increase linearly with depth from 2 m (140 ± 35 yr BP) to 7.5 m (2330 ± 30 yr BP), consistent with our age. Pine pollen collected at 11.7 m depth (the deepest depth drilled) is however much older (5460 ± 25 yr BP) and inconsistent with our results. We suggest that this pollen was derived from deposits predating the maar formation that slumped into the lake during the collapse of the crater walls. Slumps are common in the years following maar eruptions because of the instability of the steep walls (Pirrung et al., 2008). Such slumps can transform into turbidity currents when reaching the water, leaving thick deposits at the bottom of the lake, as reported for the 1977 Ukinrek maar eruption (Alaska) by Pirrung et al. (2008). Moreover, collapse and associate turbidity currents can also occur later in a maar lake history (Drohmann and Negendank, 1993; Pirrung et al., 2005), triggered for example by storms, heavy rains, or earthquakes (Pirrung et al., 2008), the last two being relatively frequent in the study area. Hence, older organic material

can potentially be reworked and deposited within the lake sediments long after the maar's initial formation, affecting the dating results throughout the sedimentary sequence (Pirrung et al., 2005). Based on this reasoning, we consider the 5460 ± 25 yr BP age reported by Bhattacharya et al. (2015) to be anomalous and conclude that the age of the maar is ~550 BC (~2400 yr BP), which is consistent with the steepness and absence of gullying of the inner crater walls.

Las Derrumbadas

The twin domes of Las Derrumbadas are the second youngest volcanoes in the study area and, by far, the highest and most voluminous (Figure 5i). Each has a diameter of 3.5–4.5 km. The total volume of both domes is 10–11 km³ (see volume calculation in Supplementary Material 2, available online). Material from the interior of the domes is microcrystalline, gray to pink rhyolite with small biotite and plagioclase phenocrysts and rare almandine garnet that were only observed in the southeastern dome. In general, rocks from the southeastern dome are more crystalline than those from the northwestern dome. The debris avalanche deposits that surround both domes were separated into two types by Siebe et al. (1995): Type 1 avalanches are heterolithologic and composed of stony and obsidian rhyolite with plagioclase and biotite phenocrysts, Cretaceous gray-beige limestone, black chert, and lacustrine white-gray friable limestone and mudstone; Type 2 avalanches are monolithologic and composed of gray and red oxidized stony rhyolite with plagioclase, biotite, and occasional garnet. Type 1 avalanches (first generation) were probably produced during dome growth, as the uppermost basement was lifted-up by the dome, and subsequently collapsed along with the dome carapace, whereas type 2 avalanches (second generation) occurred after dome growth, cutting through the hydrothermally altered interior (Siebe et al., 1995). Notably, type 2 avalanches were only identified at the southeastern dome that presents active fumaroles.

We identified fine-grained, stratified pyroclastic deposits that were located either directly below (site 26), or directly above (site 68) first-generation debris avalanche deposits at several locations around the domes. Characteristically, the contacts of these deposits with the debris avalanches are sharp and do not display the development of a soil in-between that would have indicated a significant time gap. These same pyroclastic deposits were found preserved on topographic obstacles that were surrounded by the avalanches. Among the obstacles were limestone ridges located to the SW (sites 20 and 71) and NW (site 30) of the southeastern dome, a prominent ridge along the Atexcac maar crater (site 27), and the nearby Las Águilas scoria cone and associated lavas (sites 28 and 66).

These pyroclastic deposits display significant lateral and vertical variations in componentry, sedimentary structures, and grain sizes, all of which are reported in Molina Guadarrama (2018). They are generally friable, fine-grained (fine ash to fine lapilli), thinly bedded (<10 cm), and locally display dune structures. The finest beds contain accretionary lapilli. Juvenile fragments (40–97 vol% of all clasts) are white to light-gray, dense-to-poorly vesiculated rhyolite and occasional micro-vesiculated pumice, both with euhedral phenocrysts of plagioclase and biotite. Lithic fragments comprise beige-brown Cretaceous limestone (0–30 vol%) and oxidized crystalline clasts with titanomagnetite and magnetite (0–10 vol%). These deposits are preliminarily interpreted to have originated from dilute pyroclastic density currents (pyroclastic surges) related to explosive (phreatomagmatic and/or magmatic) activity that occurred just prior to or, at some locations, just following dome growth and subsequent collapse.

A total of nine paleosols and charcoal samples, collected mostly below and in one case within the debris avalanche and
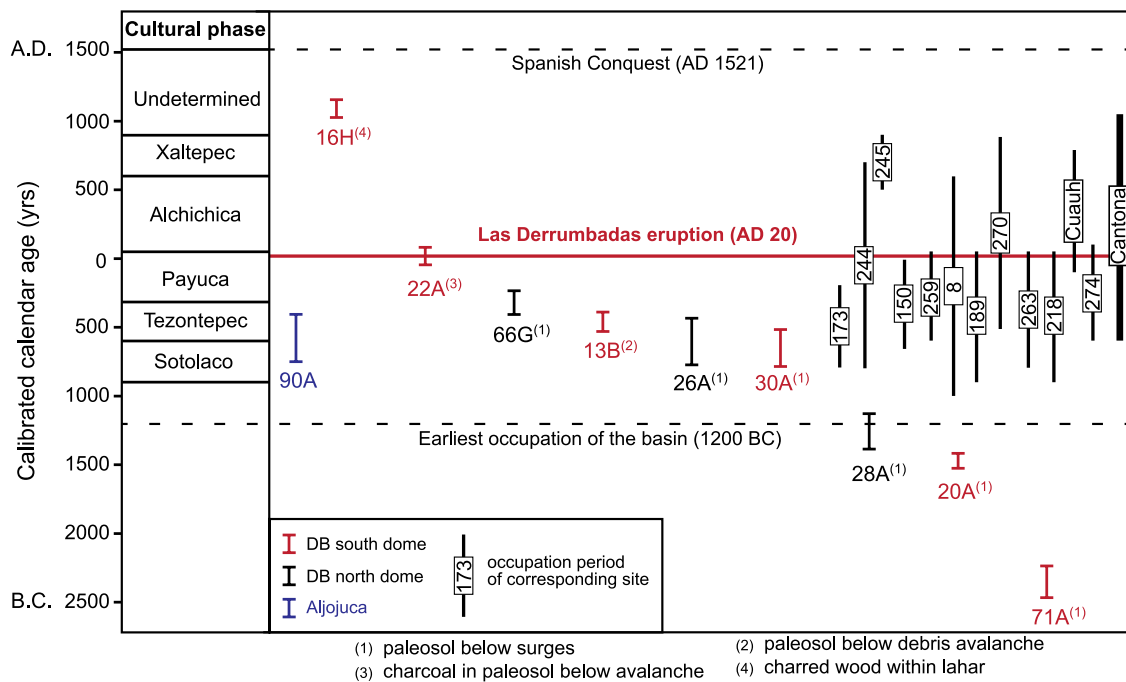
Figure 6. Graph showing calibrated radiocarbon ages for Las Derrumbadas domes (DB) and Aljojuca maar obtained in this study and their position within the archeological chart (cultural phases) established for the northern part of the Serdán-Oriental basin (García-Cook, 2009). Error bars correspond to analytical error propagated through the calibration curves from the IntCal13 database (Reimer et al., 2013). Period of occupation of several archeological sites in the region are ordered, from left to right, with increasing distance from the Las Derrumbadas domes. Cuauh stands for Cuauhyehualulco.

surge deposits at different locations around the domes, were dated to constrain the age of Las Derrumbadas domes (Table 2, Figure 6). Ages range from 2350 BC to AD 1090 and are younger than all other ages collected during this work in the central part of the basin, in full agreement with our stratigraphic reconstruction (Figure 4). These ages are younger than all previous ages reported for these domes, although relatively close to a $^{238}U/^{230}Th$ age on zircons of 4.7 ka reported by Bernal et al. (2014) (Table 1). Ages collected from the deposits related to either the southeastern and northwestern dome overlap (Figure 6), indicating that both domes could have been active at the same time. Systematic differences between ages of paleosols below surges or below debris avalanche deposits (Figure 6, Table 2) are not discernable, suggesting that no significant time had elapsed between both events.

The youngest age (AD 1090) corresponds to partially charred wood (probably burnt from a forest fire) collected at the base of a slightly indurated, very poorly sorted, massive, matrix-supported white deposit with wavy upper surface that is overlain by a 3-m-thick coarse and poorly sorted deposit probably formed by a late avalanche. The wood-bearing deposit is underlain by a 2-m-thick lahar sequence that lies unconformably above, and locally erode, a >6-m-thick sequence of surge and debris avalanche deposits (Site 16 in Figure 3 and Supplementary Material 1, available online), which indicates that it formed after a significant time gap following the main period of activity of the domes. The time gap was sufficiently long so that relatively large trees could grow on the exposed surface of the lahars. The charred trees were engulfed and buried by deposits produced by a late episode of edifice-collapse. The age of the wood should hence be considered as a minimum age for the domes.

The next youngest age is significantly older (AD 20) than the partially charred wood fragments from site 16 and was collected from charcoal fragments picked up from a paleosol exposed just below a type 1 debris avalanche deposit (site 22, Supplementary Material 1, available online). Charcoal usually yields more precise ages than bulk paleosol samples as the latest correspond to an average age of the whole carbon fraction in the sample while the

charcoal only record the age of a single dead plant. We consider this last age to be more reliable for the corresponding avalanche and thus for the eruption itself (see above). It is slightly younger than four paleosols with close ages (from 320 to 650 BC; Table 2), whereas the three oldest ages depart significantly from most of these ages, and are thus considered as anomalous and probably contaminated by older carbon. Based on these observations, we conclude that the Las Derrumbadas domes were formed just after AD 20.

Piedras Negras

The Piedras Negras lava flow covers a debris avalanche from the southeastern Las Derrumbadas dome (Figure 2) and hence represents the youngest eruption in the study area. It is 40-m-thick, blocky and andesitic (Siebe and Verma, 1988), and contains plagioclase (<2 cm), hornblende (<3 cm), few clinopyroxene, as well as abundant xenoliths. Skeletal hornblende crystals are surrounded by oxide-rims. The rough surface of the lava is still largely devoid of soil and only scarcely vegetated by few cacti and thorny bushes (Figure 5h). The lava flow is probably older than the arrival of the Spaniards in AD 1521 in the area, since its eruption is to our knowledge not reported in any colonial chronicle. Hence, Piedras Negras eruption must have occurred between AD 20 and 1521.

Discussion

Reappraisal of the ages of the recent volcanic eruptions in the region and implications for hazards

The ages obtained during this study are significantly younger than previously reported $^{40}K/^{39}Ar$ and $^{40}Ar/^{39}Ar$ dates, but consistent with a recent $^{238}U/^{230}Th$ age on zircons for Las Derrumbadas by Bernal et al. (2014) and one radiocarbon age for Aljojuca reported by De León-Barragán (2016) (Table 1). Our ages are strongly supported by the reconstructed stratigraphy in the area (Figure 4), and imply that the area has been highly active during the last 27,000 years.

For example, $^{40}K/^{39}Ar$ dating of Las Derrumbadas (Yáñez-García and García-Durán, 1982) gave a middle Pleistocene age while $^{40}Ar/^{39}Ar$ dating on glass from Tepexitl and sanidine from Cerro Pinto yielded ages of ~29 ka and 62 ka, respectively, all of which are much older than our radiocarbon ages. The inconsistency of the $^{40}Ar/^{39}Ar$ ages can be attributed to the method itself since it is inherently not always suitable for dating young samples (late Pleistocene and Holocene) because the half-life of ^{40}K is very long ($t_{1/2} = 1.25 \times 10^9$ years). Hence, few radiogenic Ar (^{40}Ar) has accumulated in young samples. As a result, even a slight contamination (excess Argon) of the sample or small analytical error can have large repercussions and produce a significant error in the obtained age (Kelley, 2002; Renne et al., 1997; Yang et al., 2014). This effect is even more pronounced for samples with low initial potassium, as is the case of the dated glass sample from Tepexitl (Ross et al., 2017). Although K-feldspars are generally less susceptible to dating errors because they are rich in potassium, they may contain microscopic melt inclusions (Esser et al., 1997) that could release their Ar at a similar temperature as the crystals. This negative effect would not be detected by the step-heating method (Kelley, 2002).

Errors in the age can also stem from the contamination of the magma by xenocrysts incorporated during partial assimilation/disintegration processes prior to eruption (Heizler et al., 1999; Yang et al., 2014) or from conduit erosion during the eruption (Chen et al., 1996; Spell et al., 2001). If dated, these xenocrysts yield ages that are older than the date of the eruption itself (Yang et al., 2014). Dated sanidines from the domes of Las Derrumbadas (Yáñez-García and García-Durán, 1982) and Cerro Pinto (Zimmer et al., 2010) may include xenocrysts derived from the underlying basement rocks.

Our chronology shows that at least 10 monogenetic volcanoes formed during the past 27,000 years, including eight during the Holocene, in the central part of the lacustrine Serdán-Oriental basin. Most of the magma extruded was rhyolitic (Cerro Pinto, Tepexitl, Las Derrumbadas) with lesser volumes of basalt to basaltic-andesitic compositions (Alchichica, Atexcac, Aljojuca, Cerro El Brujo, Tecuitlapa). Piedras Negras andesitic lava flow could not be dated in this study because it has not been quarried down so that its paleosol is not exposed. In addition, a related ash fallout layer was not found. However, its stratigraphic position above one of the Las Derrumbadas debris avalanche deposits, as well as the lack of soil and vegetation on its surface, both indicate that it represents the youngest eruption in this area (Figure 4), which must have occurred between AD 20 and 1521.

These results confirm that the region has had recent volcanic activity and that a potential eruption in the near future can occur. This would endanger several villages and the Highway 140 (Figure 2), one of the main arteries connecting ports on the Gulf of Mexico with the capital and the center of the country.

Las Derrumbadas: Eruption duration, style, and implication for hazards

The lack of paleosols between the different deposits of Las Derrumbadas is in agreement with a monogenetic nature of the domes, as postulated by Siebe et al. (1995). An exception is the presence of late avalanche deposits whose age (AD 1090) is much younger than paleosols below early surge and first-generation debris avalanche deposits, indicating that dome instability persisted much after the eruption. Stratigraphic observations indicate that first-generation avalanches formed during dome growth or soon after, as they were directly preceded and, in some places, closely followed by surges. Explosive magmatic or phreatomagmatic phases preceding dome extrusion is a common feature in other volcanic fields (e.g. Bacon et al., 1981; Fink and Pollard, 1983; Mastin and Pollard, 1988). At Las Derrumbadas,

most of the volume was erupted effusively suggesting that the magma had mostly degassed before reaching the surface. The overlap in paleosol ages obtained below deposits from both domes suggests that their age is not significantly different and that they probably erupted simultaneously or with a very short break time in-between. However, a more detailed stratigraphic study on products from the domes should be conducted to properly answer this question.

Because very few active rhyolite lava domes have been observed (Pallister et al., 2013) and none of these were monogenetic or had a size comparable to that of Las Derrumbadas, the total duration of this eruption can only be crudely estimated. Recent andesitic to rhyolitic dome eruptions had mean extrusion rates ranging from 1 to 50 m³/s (Pallister et al., 2013). During the Chaitén 2008–2010 eruption, the only rhyolite dome eruption directly witnessed in recent historic time, the dome grew during the first 4 months of the eruption by an average of 45 m³/s but the extrusion rate strongly decreased after this initial episode, including a period of inactivity, and the mean extrusion rate for the whole eruption was estimated at only 16 m³/s. This supports the idea that dome extrusion is rarely a continuous event (Calder et al., 2015) and it is likely that, for very voluminous domes, several pauses or drastic reductions of the extrusion rate can occur, as well as destructive episodes including dome collapse/explosions or debris avalanches that would delay the growth process. In general, long-duration andesitic-dacitic dome eruptions (e.g. Santiaguito in Guatemala; Rose, 1972) observed during the last century were characterized by mean extrusion rates of <5 m³/s, suggesting that an eruption such as Las Derrumbadas could last at least several decades.

Such a long duration would have implications on hazard management as highly destructive pyroclastic density currents and debris avalanches could occur during the entire period of activity, threatening the surrounding population. In the case of Las Derrumbadas, an area of >225 km² is covered by the domes and their avalanche deposits which makes this type of monogenetic activity much more hazardous than the more common monogenetic scoria cone or maar eruptions. Moreover, debris avalanches can still occur long after the dome activity has ceased and still represent a threat, as in the case of Las Derrumbadas, where an active hydrothermal system (observable on the southeast dome) and intense quarrying are further weakening both edifices.

Significance of Las Derrumbadas in volcanology

Monogenetic fields consist mostly of small volume (typically <1 km³) mafic scoria cones and fewer maars (De Silva and Lindsay, 2015). Monogenetic domes formed during a single eruption and unrelated to a polygenetic structure (e.g. stratovolcano or resurgent caldera), are comparatively uncommon on Earth. Table 3 presents a compilation of voluminous silicic dome occurrences worldwide. Most of these are associated to caldera systems such as the Mono-Inyo dome chain in the Long Valley caldera, US (Hildreth, 2004; Miller, 1985), Glass and Little Glass mountains around Medicine lake volcano, US (Fink and Pollard, 1983), or the Haroharo linear vents in the Okataina Volcanic Centre, NZ (Smith et al., 2006). However, some of these domes are located in silicic volcanic fields that have, apparently, no direct relation to caldera systems. This is for example the case of the Taylor Creek Rhyolite, US (Duffield et al., 1995), the Coso Volcanic Field, US (Bacon et al., 1981), and the Kozu-Shima island, Japan (Noguchi et al., 2006). Our case, Las Derrumbadas, is located ~50 km from the closest caldera, Los Humeros (21×14 km in diameter). Such a long distance suggests that no direct relation exists between both magmatic systems.

In terms of volume, Las Derrumbadas eruption (>10 km³) is exceptionally large for a single silicic effusive event (Table 3). Large volumes of silicic magma generally undergo violent

Table 3. Compilation of data for large silicic domes reported in the literature.

Dome(s) or calderic system name	Age	Magma type (wt% SiO$_2$)	Maximum volume of a single dome (km^3)	Largest volume of silicic lava emitted by one eruption (km^3)	Reference
Inyo Chain, California, US	6–0.55 ka	Rhyolite (70–74%)	0.17	<0.5	Miller (1985), Sampson and Cameron (1987)
Mono chain, California, US	55–0.66 ka	Dacite (67–69%) Rhyolite (76–77%)	<0.5	~0.5	Hildreth (2004), Sieh and Bursik (1986)
Kozu-shima, Japan[a]	>1.1 ka	Rhyolite (74–77%)	1–2	1–2	Noguchi et al. (2006)
Nii Jima, Japan[a]	>1.16 ka	Rhyolite (76–78%)	<1	<1	Koyaguchi (1986)
Little Glass and Glass Mountains, California, US	>1.1 ka	Mainly rhyolite (73.5–74%)	<1	<1.5	Fink and Pollard (1983), Heiken (1978)
Las Derrumbadas, Mexico[a]	**2 ka**	**Rhyolite (70.5–76%)**	**5.33**	**>10.6**	**This study**
Kikai, Japan	<7.3 ka	Rhyolite (68–72%)	32	32	Tatsumi et al. (2018)
Whakatane, Okataina, NZ	5.6 ka	Rhyolite (73–76%)	0.85	8	Smith et al. (2006)
Mamaku, Okataina, NZ	8.1 ka	Rhyolite (76–77%)	0.69 lava flow: 4.08	12	Smith et al. (2006)
Salton Buttes, California US[a]	<10 ka	High-K rhyolite (73.2–76.4%)	~1	~1	Wright et al. (2015)
Olkaria, Kenya	22 ka–present	Peralkaline rhyolite, trachyte, comendite	<1	<1	MacDonald et al. (2008)
Acigöl rhyolite field, Turkey	180–20 ka	Alkaline rhyolite (74–77%)	0.25	0.25	Druitt et al. (1995)
La Primavera, Jaliscco, Mexico	145–25 ka	Rhyolite (>75%)	0.8	0.8	Mahood (1981)
Coso Volcanic Field, California, US[a]	4 Ma–40 ka	Rhyolite (~77%)	0.3	0.3	Bacon et al. (1981), Bacon (1982)
High lava plain, Oregon, US[a]	12 Ma–present	Rhyolite	>1	>1	Ford et al. (2013)
Cerro Chascon, APVC, Bolivia	85 ka	Dacite (~68%)	4.9	4.9	Watts et al. (1999), Tierney et al. (2016)
Cerro Chillahuita, APVC, Chile	107.8 ± 6.4 ka	Dacite (~69%)	4	4	De Silva et al. (1994), Tierney et al. (2016)
Cerro Tocopuri, APVC, Chile	110.3 ± 3.4 ka	Rhyolite (~71.5%)	4	4	De Silva et al. (1994), Tierney et al. (2016)
Chao lava flow, APVC, Chile	111.2 ± 7.5 ka	Dacite (~68%)	22.5 (lava flow)	22.5	De Silva et al. (1994), Tierney et al. (2016)
Cerro Chanca, APVC, Chile	119.8 ± 5.4 ka	Dacite (~65%)	4–5	4–5	De Silva et al. (1994), Tierney et al. (2016)
Taylor Creek Rhyolite, New Mexico, US[a]	27.9 Ma	Rhyolite (77.5%)	10	10	Duffield et al. (1995)

[a]Monogenetic fields or edifices not directly related to a caldera system.
'x' = unknown.

shallow fragmentation that leads to explosive eruptions, at least in the early eruptive phases (Eichelberger, 1995; Fink et al., 1992; Jaupart and Allègre, 1991). In the Holocene, the Mamaku and Whakatane eruptions from the Okataina volcanic zone, NZ, emitted respectively 13 km^3 and 11.3 km^3 of rhyolite magma, most of it effusively. However, these eruptions created several domes that are individually quite small (<1 km^3). Domes of similar size as Las Derrumbadas have been described in the Altiplano-Puna volcanic region in the Central Andes, including four late-Pleistocene (~120–110 ka) domes of more than 4 km^3 each and a >22 km^3 lava flow (Chao dacite, De Silva et al., 1994). From the Tertiary Taylor Creek Rhyolite, New Mexico, Duffield et al. (1995) report a dome with a volume of 10 km^3. To our knowledge, the largest (32 km^3) single lava dome ever reported is actively being extruded inside the subaquatic Kikai caldera following a large (500 km^3) ignimbritic eruption that occurred at 7.3 ka (Tatsumi et al., 2018).

In Mexico, Las Derrumbadas is not the only recent large-volume monogenetic eruption. In Michoacán, >9 km^3 of andesitic lava were emitted during a single eruption in the late Holocene, forming El Metate shield volcano (Chevrel et al., 2016). This suggests that, at least in Mexico, monogenetic eruptions are not as small as commonly thought, which should be considered for hazard assessments in monogenetic fields.

Implications for archeological studies

The late-Holocene age of Las Derrumbadas domes revealed by this study indicates that the eruption may have been witnessed by pre-Hispanic populations inhabiting the Serdán-Oriental basin and could have had an impact on their development. Around 1200 BC, the population was scattered in small agricultural settlements built on elevated landforms across the basin (Gazzola, 2005). At ~600 BC, the population in the basin had significantly increased and groups began to settle in the area of Cantona on the lavas of Los Humeros caldera (Carrasco-Núñez et al., 2018; García-Cook, 2009) (Figure 1). At the start of the Payuca period (300 BC–AD 50), ~60,000 people were living in small villages while ~28,000 people were living in Cantona (García-Cook, 2009). At 200 BC, small sites started to be abandoned, and this process intensified in the 50 BC to AD 50 period (Figure 6). At AD 50, from the 160 archeological sites occupied at the start of the Payuca period, 88 were abandoned, and the total population in the villages was reduced to one-half (<30,000 inhabitants). Meanwhile, the population in Cantona almost doubled (~52,000 inhabitants) and another city, Cuauhyehualulco, was established in the southern-central part of the basin, on the lava from Cerro El Brujo (Figure 2) (García-Cook Zamora-Rivera, 2010). So far, no straightforward hypothesis has been proposed to explain this rapid migration of populations from small rural villages to larger urban sites.
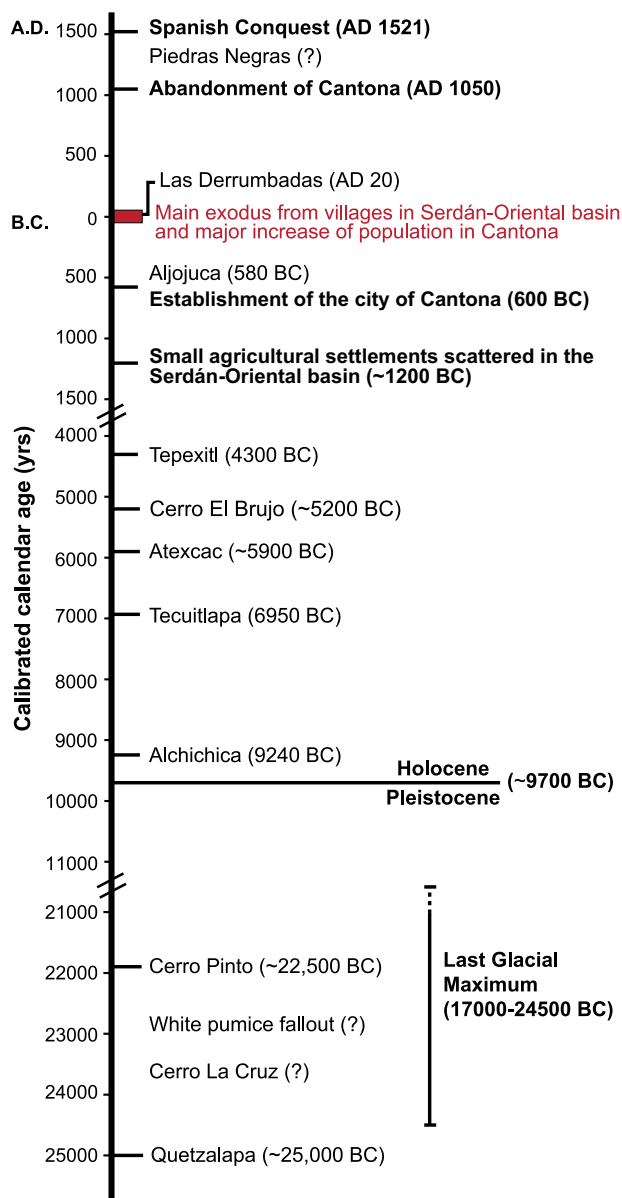
Figure 7. Chronological graph for the Serdán-Oriental basin depicting known volcanic eruptions during the last 27,000 years. Major geologic events and important social developments are indicated in bold. Last Glacial Maximum time range after Clark et al. (2009).

Interestingly, the migration peak period (50 BC to AD 50) overlaps with our age estimate for the eruption of Las Derrumbadas within margins of error (45 BC–AD 85, Figures 6 and 7). Considering the large size of the Las Derrumbadas domes, the broad area covered by its deposits (~225 km²), and the violent eruption mechanisms that preceded and accompanied their emplacement (surges and avalanches), it seems likely that people living in nearby rural communities became frightened and abandoned their villages. In fact, most of the archeological sites of the Payuca period that are close to Las Derrumbadas were deserted (Figures 2 and 6). One notable exception is archeological site 244 located on Cerro Pinto, which was occupied until AD 700 (Jiménez-Reyes et al., 2016; Téllez-Nieto, 2013). The location of this site 200 m above the lacustrine plain, within a tuff ring and behind the domes of Cerro Pinto (Figure 2) might have protected the population from the impacts of the eruption and allowed them to pursue their activities. The sites of Cantona and Cuauhyehualulco, to which most of the population fled, were located at distances of 20 and 28 km, respectively, probably sufficiently far and

safe from the eruption site. Hence, it is our hypothesis that the eruption of Las Derrumbadas could have contributed to the rapid rural exodus and subsequent urban nucleation in Cantona and Cuauhyehualulco that occurred ~2000 years ago in the Serdán-Oriental basin.

Relevance for studies on the timescale of species evolution in maar lakes

Because they start as 'virgin' habitats and are relatively isolated from their surroundings, crater lakes are of great interest for biologists and limnologists trying to investigate the colonization and diversification of species living in young ecosystems (Elmer et al., 2010, 2013; Percino-Daniel et al., 2016). The study area includes several maar lakes of interest for such studies. Alchichica and Atexcac have attracted particular interest because they are both filled with brackish alkaline water with a pH of ~9 (Kaźmierczak et al., 2011). Both lakes are ~10 km apart from each other and Atexcac's lake surface is ~40 m higher than Alchichica's indicating that they might not share the same aquifer and are hence not directly connected. Despite the rather extreme water chemistry, several species have colonized the lakes and diversified to adapt to these unusual conditions. In particular, Alchichica shows a large diversity of fauna and harbors several endemic species that range from microscopic in size such as diatoms, to larger animals like fishes and amphibians (Suárez-Morales et al., 2013).

The young age of the maars in the basin revealed by this study sheds new light on these processes, implying that the development of such biodiversity must have occurred relatively fast, over only a few 1000 years. An interesting case of species evolution concerns the salamanders that are present as two main species in the area. While *Ambystoma velasci* is present in several lakes in the area (Tecuitlapa, Atexcac, Quechulac, and La Mina – or La Preciosa; Percino-Daniel et al., 2016), *Ambystoma taylori* is endemic to Alchichica and displays characteristics that are specific to the lake conditions (Brandon et al., 1981; Percino-Daniel et al., 2016). Because *Ambystoma taylori* is morphologically very similar to the local populations of *Ambystoma velasci*, it is believed to have diversified from the latter (Brandon et al., 1981; Percino-Daniel et al., 2016; Shaffer, 1984). In Atexcac, *Ambystoma velasci* displays some adaptations to the lake conditions but has not yet differentiated entirely to a new species. Several hypotheses have been put forward to explain these differences, but we propose that the younger age of Atexcac maar (5960 BC) compared with Alchichica (9240 BC) could account for the shorter time available for the genetic evolution of the salamander. Note that the colonization of the lakes does not necessary occur immediately after the eruption, depending on various parameters such as their geographical location (e.g. proximity to other water bodies), climate, configuration of the crater (e.g. rim height), and remnant activity of the volcano (e.g. duration of degassing after the eruption) (Elmer et al., 2010). Hence, the time available for the evolution of species should be shorter than the age of the maars.

Conclusion

Radiocarbon ages obtained in this study revealed that the central part of the Serdán-Oriental basin was very active in the last 27,000 years with the formation of at least 10 monogenetic edifices, eight of which being Holocene in age (Alchichica, Tecuitlapa, Atexcac, Cerro El Brujo, Tepexitl, Aljojuca, Las Derrumbadas, and Piedras Negras).

Some of the ages reported here are significantly younger than previously estimated, indicating that the ⁴⁰K/³⁹Ar and ⁴⁰Ar/³⁹Ar dating techniques are of limited use in this area, especially when trying to date very young eruptions. In contrast, our new age

estimate for the Las Derrumbadas domes (AD 20) is consistent with, although younger than a recent $^{238}U/^{230}Th$ age on zircons. This eruption may have lasted decades, causing significant impact in the region. Its age coincides with a period marked by a migration of pre-Hispanic populations from small rural hamlets in the center of the basin to large cities located more than 20 km from the eruption site (García-Cook, 2009), suggesting a possible causal link between the Las Derrumbadas eruption and a major episode of human migration in eastern-central Mexico. The young ages reported for the maars suggest that the isolated aquatic ecosystems that developed in their respective crater lakes may have evolved rapidly creating a unique diversity of species, especially in the case of Alchichica. These findings stress the need for further archeological, biological, and geochronological research in the area.

The extrusion of Las Derrumbadas domes is by far the most voluminous Holocene eruption in the area and represents also one of the most voluminous Holocene silicic effusive eruptions worldwide. Overlaps in the radiocarbon ages as well as field evidence support the idea that the large domes ($>$5 km³ each) were extruded in a single eruptive event. Such large monogenetic eruptions should be accounted for when assessing potential hazards in monogenetic fields. In particular, Las Derrumbadas domes are likely to collapse further in the future, hence threatening the population living and working at large quarries in the area. Moreover, as the volcanic activity in this part of the basin has been relatively intense during the Holocene a new eruption is likely to occur during the next few 1000 years.

ORCID iD

Corentin Chédeville https://orcid.org/0000-0002-1078-7391

Supplemental material

Supplemental material for this article is available online.

References

Acosta R, Prat N, Ribera C et al. (2017) Chironomus alchichica sp. n. (Diptera: Chironomidae) from Lake Alchichica, Mexico. *Zootaxa* 4365(1): 53–70.

Austin-Erickson A, Ort MH and Carrasco-Núñez G (2011) Rhyolitic phreatomagmatism explored: Tepexitl tuff ring (Eastern Mexican Volcanic Belt). *Journal of Volcanology and Geothermal Research* 201(1–4): 325–341.

Bacon CR (1982) Time-predictable bimodal volcanism in the Coso Range, California. *Geology* 10(2): 65–69.

Bacon CR, Macdonald R, Smith RL et al. (1981) Pleistocene high-silica rhyolites of the Coso volcanic field, Inyo County, California. *Journal of Geophysical Research* 86(B11): 10223–10241.

Bernal JP, Solari LA, Gómez-Tuena A et al. (2014) In-situ 230Th/U dating of Quaternary zircons using LA-MCICPMS. *Quaternary Geochronology* 23: 46–55.

Bhattacharya T, Byrne R, Böhnel H et al. (2015) Cultural implications of late-Holocene climate change in the Cuenca Oriental, Mexico. *Proceedings of the National Academy of Sciences* 112(6): 1693–1698.

Bloomfield K (1975) A late-Quaternary monogenetic volcano field in central Mexico. *Geologische Rundschau* 64(1): 476–497.

Brandon RA, Maruska EJ and Rumph WT (1981) A new species of neotenic Ambystoma (Amphibia, Caudata) endemic to Laguna Alchichica, Puebla, Mexico. *Bulletin of the Southern California Academy of Sciences* 80(3): 112–125.

Burkart JH (1867.) *Nähere Angaben über die Fundorte des Domeykits und der Manganblende in Mexico* (The Preciosa Sangre de Cristo deposit (Puebla 4)). New York: Neues Jahrbuch, pp. 826–828.

Calder ES, Lavallée Y, Kendrick JE et al. (2015) Lava dome eruptions. In: Sigurdsson H, Houghton B, Rymer H et al. (eds) *The Encyclopedia of Volcanoes*. New York: Springer, pp. 343–362.

Carrasco-Núñez G and Riggs NR (2008) Polygenetic nature of a rhyolitic dome and implications for hazard assessment: Cerro Pizarro volcano, Mexico. *Journal of Volcanology and Geothermal Research* 171(3–4): 307–315.

Carrasco-Núñez G and Rose WI (1995) Eruption of a major Holocene pyroclastic flow at Citlaltepetl. *Journal of Volcanology and Geothermal Research* 69: 197–215.

Carrasco-Núñez G, Ort MH and Romero C (2007) Evolution and hydrological conditions of a maar volcano (Atexcac crater, Eastern Mexico). *Journal of Volcanology and Geothermal Research* 159(1–3): 179–197.

Carrasco-Núñez G, Bernal JP, Dávila P et al. (2018) Reappraisal of Los Humeros volcanic complex by new U/Th zircon and $^{40}Ar/^{39}Ar$ dating: Implications for greater geothermal potential. *Geochemistry Geophysics Geosystems* 19: 132–149.

Carrasco-Núñez G, Dávila-Harris P, Ort MH et al. (2012) Recent explosive volcanism at the eastern Trans-Mexican Volcanic Belt. In: Aranda-gómez JJ, Tolson G, and Molina-garza RS (eds) *The Southern Cordillera and beyond: Geological Society of America Field Guide 25*. Boulder, CO: The Geological Society of America, pp. 83–113.

Castro-Govea R and Siebe C (2007) Late Pleistocene-Holocene stratigraphy and radiocarbon dating of La Malinche volcano, Central Mexico. *Journal of Volcanology and Geothermal Research* 162(1–2): 20–42.

Chen Y, Smith PE, Evensen NM et al. (1996) The edge of time: Dating younger volcanic ash layers with the ^{40}Ar-^{39}Ar laser probe. *Science* 274: 1176–1178.

Chevrel MO, Siebe C, Guilbaud M-N et al. (2016) The AD 1250 El Metate shield volcano (Michoacán): Mexico's most voluminous Holocene eruption and its significance for archaeology and hazards. *The Holocene* 26(3): 471–488.

Clark PU, Dyke AS, Shakun JD, et al. (2009) The last glacial maximum. *Science* 325(5941): 710–714. DOI: 10.1126/science.1172873.

Couradeau E, Benzerara K, Gérard E et al. (2012) An early-branching microbialite cyanobacterium forms intracellular carbonates. *Science* 336(6080): 459–462.

de Buen F (1945) Investigaciones sobre ictiología Mexicana. I. Atherenidae De Aguas Continentales De México. *Anales Del Instituto De Biología De La Universidad Nacional Autónoma De México* 16: 475–532.

De León-Barragán L (2016) *Estratigrafía y evolución del volcán tipo maar (axalapazco) Aljojuca, Puebla*. MSc Thesis,

UNAM, p. 168. Available at: http://www.lareferencia.info/vufind/Record/MX_3cbb8862e38d9a46ef8892a436bdd165

De Silva SL and Lindsay JM (2015) Primary volcanic landforms. In: Sigurdsson H, Houghton B, Rymer H et al. (eds) *The Encyclopedia of Volcanoes*. New York: Springer, pp. 273–297.

De Silva SL, Self S, Francis PW et al. (1994) Effusive silicic volcanism in the Central Andes: The Chao dacite and other young lavas of the Altiplano-Puna Volcanic Complex. *Journal of Geophysical Research* 99(B9): 17805–17825.

Drohmann D and Negendank JFW (1993) Turbidites in the sediments of lake Meerfelder Maar (Germany) and the explanation of suspension sediments. *Paleolimnology of European Maar Lakes* 49: 193–208.

Druitt TH, Brenchley PJ, Gokten YE et al. (1995) Late Quaternary rhyolitic eruptions from the Acigol Complex, central Turkey. *Journal of the Geological Society* 152(4): 655–667.

Duffield BW, a Richter DH and Priest SS (1995) Physical volcanology of silicic lava domes as exemplified by the Taylor Creek Rhyolite, Catron and Sierra Counties, New Mexico. U.S. Geological Survey Map I-2399, 1:50,000, pp. 1–16. Available at: https://pubs.usgs.gov/imap/2399/report.pdf

Eichelberger JC (1995) Silicic volcanism: Ascent of viscous magmas from crustal reservoirs. *Annual Review of Earth and Planetary Sciences* 23: 41–63.

Elmer KR, Lehtonen TK, Fan S et al. (2013) Crater lake colonization by neotropical cichlid fishes. *Evolution* 67(1): 281–288.

Elmer KR, Lehtonen TK, Kautt AF et al. (2010) Rapid sympatric ecological differentiation of crater lake cichlid fishes within historic times. *BMC Biology* 8: 60.

Escobar-Briones E and Alcocer J (2002) Caecidotea williamsi (Crustacea: Isopoda: Asellidae), a new species from a saline crater-lake in the eastern Mexican Plateau. *Hydrobiologia* 477: 93–105.

Esser RP, McIntosh WC, Heizler MT et al. (1997) Excess argon in melt inclusions in zero-age anorthoclase feldspar from Mt. Erebus, Antarctica, as revealed by the method. *Geochimica et Cosmochimica Acta* 61(18): 3789–3801.

Ferriz H and Mahood GA (1984) Eruption rates and compositional trends at Los Humeros Volcanic Center, Puebla, Mexico. *Journal of Geophysical Research* 89(B10): 8511.

Fink JH and Pollard DD (1983) Structural evidence for dikes beneath silicic domes, Medicine Lake Highland Volcano, California (USA). *Geology* 11(8): 458–461.

Fink JH, Anderson SW and Manley CR (1992) Textural Constraints on Effusive Silicic Volcanism: Beyond the Permeable Foam Model. *Journal of Geophysical Research* 97(B6): 9073–9083.

Ford MT, Grunder AL and Duncan RA (2013) Bimodal volcanism of the high lava plains and Northwestern Basin and Range of Oregon: Distribution and tectonic implications of age-progressive rhyolites. *Geochemistry, Geophysics, Geosystems* 14(8): 2836–2857.

García-Cook Á (2009) El Formativo en la mitad norte de la Cuenca de Oriental. *Arqueología* 40: 115–152.

García-Cook Á and Zamora-Rivera ÁM (2010) Las canchas de Juego de Pelota de Cuauhyehualulco, Puebla, y la importancia de éste en la 'Ruta comercial Golfo-Sur al Altiplano Central'. *Arqueología* 43: 115–135.

Gazzola J (2005) Avances y resultados preliminares del Proyecto Norte de la Cuenca de Oriental, Puebla. *Arqueología* 35: 50–67.

Gérard E, Ménez B, Couradeau E et al. (2013) Specific carbonate-microbe interactions in the modern microbialites of Lake Alchichica (Mexico). *The ISME Journal* 7(10): 1997–2009.

Guilbaud MN, Siebe C, Layer P et al. (2011) Geology, geochronology, and tectonic setting of the Jorullo Volcano region, Michoacán, México. *Journal of Volcanology and Geothermal Research* 201: 97–112.

Guilbaud MN, Siebe C, Layer P et al. (2012) Reconstruction of the volcanic history of the Tacámbaro-Puruarán area (Michoacán, México) reveals high frequency of Holocene monogenetic eruptions. *Bulletin of Volcanology* 74(5): 1187–1211.

Hasenaka T and Carmichael ISE (1985) The cinder cones of Michoacán-Guanajuato, central Mexico: Their age, volume and distribution, and magma discharge rate. *Journal of Volcanology and Geothermal Research* 25(1–2): 105–124.

Heiken G (1978) Plinian-type eruptions in the medicine lake highland, california, and the nature of the underlying magma. *Journal of Volcanology and Geothermal Research* 4(3–4): 375–402. DOI: 10.1016/0377-0273(78)90023-9.

Heizler MT, Perry FV, Crowe BM et al. (1999) The age of Lathtop Wells volcanic center : An 40Ar /39Ar dating investigation surface. *Journal of Geophysical Research* 104(B1): 767–804.

Hildreth W (2004) Volcanological perspectives on long valley, Mammoth Mountain, and Mono Craters: Several contiguous but discrete systems. *Journal of Volcanology and Geothermal Research* 136(3–4): 169–198.

Hoskuldsson A and Robin C (1993) Late Pleistocene to Holocene eruptive activity of Pico de Orizaba, Eastern Mexico. *Bulletin of Volcanology* 55(8): 571–587.

Jansson A (1979) A new species of Krizousacorixa from Mexico (Heteroptera, Corixidae). *The Pan-pacific Entomologist* 55: 258–260.

Jaupart C and Allègre CJ (1991) Gas content, eruption rate and instabilities of eruption regime in silicic volcanoes. *Earth and Planetary Science Letters* 102(3–4): 413–429.

Jiménez-Reyes AL, Téllez-Nieto AL, García-Cook Á et al (2016) Obsidiana arqueologica de Cantona, Puebla: Los diversos orígenes. *Arqueologia* 51: 134–152.

Kaźmierczak J, Kempe S, Kremer B et al. (2011) Hydrochemistry and microbialites of the alkaline crater lake Alchichica, Mexico. *Facies* 57(4): 543–570.

Kelley S (2002) Excess argon in K-Ar and Ar-Ar geochronology. *Chemical Geology* 188(1–2): 1–22.

Koyaguchi T (1986) Evidence for two-stage mixing in magmatic inclusions and rhyolitic lava domes on Niijima Island, Japan. *Journal of Volcanology and Geothermal Research* 29(1–4): 71–98.

MacDonald R, Belkin HE, Fitton JG et al. (2008) The roles of fractional crystallization, magma mixing, crystal mush remobilization and volatile-melt interactions in the genesis of a young basalt-peralkaline rhyolite suite, the greater Olkaria volcanic complex, Kenya Rift valley. *Journal of Petrology* 49(8): 1515–1547.

Mahood GA (1981) A summary of the geology and petrology of the Sierra La Primavera, Jalisco, Mexico. *Journal of Geophysical Research* 86(B11): 10137–10152.

Mastin LG and Pollard DD (1988) Surface deformation and shallow dike intrusion processes at Inyo Craters, Long Valley, California. *Journal of Geophysical Research: Solid Earth* 93(B11): 13221–13235.

Matthews JA (1985) Radiocarbon dating of surface and buried soils: Principles, problems and prospects, Geomorphology and soils. In: *Proceedings of the association with a conference of the British geomorphological research group* (eds KS. Richards, RR. Arnett and S. Ellis), University of Hull, Hull, 28–30 September. London: G. Allen & Unwin.

Miller CD (1985) Holocene eruptions at the Inyo volcanic chain, California: Implications for possible eruptions in Long Valley caldera. *Geology* 13(1): 14–17.

Molina Guadarrama AN (2018) Oleadas piroclásticas de Las Derrumbadas (Puebla, México): Estructuras, componentes y procesos de formación. *Tesis De Licenciatura, Facultad De Ingeniería, UNAM, p.* 89.

Montiel-Martínez A, Ciros-Pérez J, Ortega-Mayagoitia E et al. (2008) Morphological, ecological, reproductive and molecular evidence for Leptodiaptomus garciai (Osorio-Tafall 1942) as a valid endemic species. *Journal of Plankton Research* 30(10): 1079–1093.

Negendank JFM, Emmermann R and Krawczyk R (1985) Geological and geochemical investigations on the eastern trans-Mexican Volcanic Belt. *Geofísica Internacional* 24(4): 477–575.

Noguchi S, Toramaru A and Shimano T (2006) Crystallization of microlites and degassing during magma ascent: Constraints on the fluid mechanical behavior of magma during the Tenjo Eruption on Kozu Island, Japan. *Bulletin of Volcanology* 68(5): 432–449.

Oliva MG, Lugo A, Alcocer J et al. (2006) Cyclotella alchichicana sp. *Nov. from a Saline Mexican Lake. Diatom Research* 21(1): 81–89.

Ordóñez E (1905) Los Xalapascos del Estado de Puebla. 1a Parte. *Paregones Del Instituto Geológico De México* 1: 295–393.

Ordóñez E (1906) Los Xalapascos del Estado de Puebla. 2a Parte. *Paregones Del Instituto Geológico De México* 1(8): 348–405.

Ort MH and Carrasco-Núñez G (2009) Lateral vent migration during phreatomagmatic and magmatic eruptions at Tecuitlapa Maar, east-central Mexico. *Journal of Volcanology and Geothermal Research* 181(1–2): 67–77.

Palacios D and Vazquez-Selem L (1996) Geomorphic Effects of the Retreat of Jamapa Glacier, Pico de Orizaba Volcano (Mexico). *Geografiska Annaler: Series A, Physical Geography* 78(1): 19–34.

Pallister JS, Diefenbach AK, Burton WC et al. (2013) The Chaitén rhyolite lava dome: Eruption sequence, lava dome volumes, rapid effusion rates and source of the rhyolite magma. *Andean Geology* 40(2): 277–294.

Pardo M and Suárez G (1995) Shape of the subducted Rivera and Cocos plates in southern Mexico: Seismic and tectonic implications. *Journal of Geophysical Research* 100(B7): 12357–12373.

Percino-Daniel R, Recuero E, Vázquez-Domínguez E et al. (2016) All grown-up and nowhere to go: Paedomorphosis and local adaptation in Ambystoma salamanders in the Cuenca Oriental of Mexico. *Biological Journal of the Linnean Society* 118(3): 582–597.

Pirrung M, Büchel G, Lorenz V et al. (2008) Post-eruptive development of the Ukinrek East Maar since its eruption in 1977 A.D in the Periglacial area of South-west Alaska. *Sedimentology* 55(2): 305–334.

Pirrung M, Schulte-Vieting U, Treutler H et al. (2005) Dating of lacustrine sediments from the tropical maar Ranu Klindungan, East Java (Indonesia). *Zeitschrift Der Deutschen Gesellschaft Für Geowissenschaften* 156(4): 557–571.

Reimer P, Bard E, Bayliss A et al. (2013) Intcal13 and marine13 radiocarbon age calibration curves 0 – 50,000 years cal bp. *Radiocarbon* 55(4): 1869–1887.

Renne PR, Sharp WD, Deino AL et al. (1997) 0Ar/39Ar dating into the historical realm : Calibration against pliny the younger. *Science* 277: 1279–1280.

Reyes-Guzmán N, Siebe C, Chevrel MO et al. (2018) Geology and radiometric dating of Quaternary monogenetic volcanism in the western Zacapu lacustrine basin (Michoacán, México): Implications for archeology and future hazard evaluations. *Bulletin of Volcanology* 80(2): 18–20.

Rodríguez SR (2005) Geology of Las Cumbres Volcanic Complex, Puebla and Veracruz states, Mexico. *Revista Mexicana De Ciencias Geologicas* 22(2): 181–198.

Rodríguez SR, Siebe C, Komorowski JC et al. (2002) The Quetzalapa Pumice: A voluminous late pleistocene rhyolite deposit in the eastern Trans-Mexican Volcanic Belt. *Journal of Volcanology and Geothermal Research* 113(1–2): 177–212.

Ross PS, Carrasco-Núñez G and Hayman P (2017) Felsic maar-diatreme volcanoes: A review. *Bulletin of Volcanology* 79(2): 20.

Rose WI (1972) Santiaguito Volcanic Dome, Guatemala. *Geological Society of America Bulletin* 83(5): 1413–1434.

Sampson DE and Cameron KL (1987) The geochemistry of the Inyo volcanic chain: Multiple magma systems in the long valley region, Eastern California. *Journal of Geophysical Research* 92(B10): 10403–10421.

Shaffer HB (1984) Evolution in a paedomorphic Lineage. I. an electrophoretic analysis of the Mexican ambystomatid salamanders. *Evolution* 38(6): 1207.

Siebe C and Verma SP (1988) Major element geochemistry and tectonic setting of Las Derrumbadas rhyolitic domes, Puebla, Mexico. *Chemie Der Erde* 48: 177–189.

Siebe C, Arana-Salinas L and Abrams M (2005) Geology and radiocarbon ages of Tláloc, Tlacotenco, Cuauhtzin, Hijo del Cuauhtzin, Teuhtli, and Ocusacayo monogenetic volcanoes in the central part of the Sierra Chichinautzin, México. *Journal of Volcanology and Geothermal Research* 141(3–4): 225–243.

Siebe C, Abrams M, Macías JL et al. (1996) Repeated volcanic disasters in Prehispanic time at Popocatépetl, central Mexico: Past key to the future? *Geology* 24(5): 399–402.

Siebe C, Macías JL, Abrams M et al. (1995) Quaternary explosive volcanism and pyroclastic deposits in east central Mexico: Implications for future hazards. *Geological Society of America Annual Meeting 1995*. New Orleans, LA: Field Trip Guide Book 1, p. 47.

Siebe C, Rodríguez-Lara V, Schaaf P et al. (2004) Radiocarbon ages of Holocene Pelado, Guespalapa and Chichinautzin scoria cones, south of Mexico City: Implications for archaeology and future hazards. *Bulletin of Volcanology* 66(3): 203–225.

Sieh K and Bursik M (1986) Most recent eruption of the Mono Craters, Eastern Central California. *Journal of Geophysical Research* 91(B12): 539–571.

Smith VC, Shane P, Nairn IA et al. (2006) Geochemistry and magmatic properties of eruption episodes from Haroharo linear vent zone, Okataina Volcanic Centre, New Zealand during the last 10 kyr. *Bulletin of Volcanology* 69(1): 57–88.

Spell TL, Smith EI, Sanford A et al. (2001) Systematics of xenocrystic contamination: Preservation of discrete feldspar populations at McCullough Pass Caldera revealed by $^{40}Ar/^{39}Ar$ dating. *Earth and Planetary Science Letters* 5890: 1–13.

Suárez-Morales E, Barrera-Moreno O and Ciros-Pérez J (2013) A new species of Cletocamptus Schmankewitsch, 1875 (Crustacea, Copepoda, Harpacticoida) from a high altitude saline lake in Central Mexico. *Journal of Limnology* 72(2): 313–325.

Tatsumi Y, Suzuki-Kamata K, Matsuno T et al. (2018) Giant rhyolite lava dome formation after 7.3 ka supereruption at Kikai caldera, SW Japan. *Scientific Reports* 8(1): 2753.

Téllez-Nieto AL (2013) Identificación de procedencia para obsidianas de Cantona, Puebla, por el método de Análisis Por Activación Neutrónica (AAN). *MSc Thesis, Escuela Nacional de Antropologia e Historia, p. 189.*

Tierney CR, Schmitt AK, Lovera OM et al. (2016) Voluminous plutonism during volcanic quiescence revealed by thermochemical modeling of zircon. *Geology* 44(8): 683–686.

van Wyk de Vries B and Davies T (2015) Landslides, debris avalanches, and volcanic gravitational deformation. In: Sigurdsson H, Houghton B, Rymer H et al. (eds) *The Encyclopedia of Volcanoes*, 2nd edn. New York: Springer, pp. 665–685.

Vázquez-Selem L and Heine K (2011) Late Quaternary Glaciation in Mexico. In: Vázquez-Selem L and Heine K (eds) *Developments in Quaternary Science*. New York: Elsevier, pp. 849–861.

Vilaclara G, Chávez M, Lugo A et al. (1993) Comparative description of crater-lakes basic chemistry in Puebla State, Mexico. *Internationale Vereinigung Für Theoretische Und Angewandte Limnologie: Verhandlungen* 25(1): 435–440.

Watts RB, De Silva SL, Jimenez De Rios G et al. (1999) Effusive eruption of viscous silicic magma triggered and driven by recharge: A case study of the Cerro Chascon-Runtu Jarita Dome Complex in Southwest Bolivia. *Bulletin of Volcanology* 61(4): 241–264.

Wohletz KH and Sheridan MF (1979) A model of pyroclastic surge. *Geological Society of America Special Paper* 180(1976): 177–193.

Wood CA (1974) Reconnaissance geophysics and geology of the Pinacate craters, Sonora, Mexico. *Bulletin Volcanologique* 38(1): 149–172.

Wright HM, Vazquez JA, Champion DE et al. (2015) Episodic Holocene eruption of the Salton Buttes rhyolites, California, from paleomagnetic, U-Th, and Ar/Ar dating. *Geochemistry, Geophysics, Geosystems* 16(4): 1198–1210.

Yáñez-García C and García Durán S (1982) *Exploración de la región geotérmica : Los Humeros-Las Derrumbadas, estados de Puebla y Veracruz*. Mexico: Comisión Federal De Electricidad, p. 96.

Yáñez-García A and Casique J (1980) *Informe geológico del proyecto geotérmico Los Humeros-Derrumbadas, estados de Puebla y Veracruz: México*. Mexico: Comisión Federal De Electricidad, p. 97.

Yang L, Wang F, Feng H et al. (2014) ^{0}Ar/^{39}Ar geochronology of Holocene volcanic activity at Changbaishan Tianchi volcano, Northeast China. *Quaternary Geochronology* 21(1): 106–114.

Zimmer BW, Riggs NR and Carrasco-Núñez G (2010) Evolution of tuff ring-dome complex: The case study of Cerro Pinto, eastern Trans-Mexican Volcanic Belt. *Bulletin of Volcanology* 72(10): 1223–1240.